



Projecting Global Population Grids to 2100: Final Report

Produced in fulfilment of the requirements specified
under contract number 2018.CE.16.BAT.0505

Bryan Jones, Deborah Balk, Stefan Leyk, Mark Montgomery, and Hasim Engin
December 2020

Table of Contents

1 BACKGROUND AND OBJECTIVES	3
1.1 Development of new spatial data products	3
2 DATA AND METHODS	4
2.1 Input data	4
2.1.1 National-level population scenarios: The shared socioeconomic pathways	5
2.1.2 The Global Human Settlement Layer (GHSL)	6
2.1.3 The Global Human Settlement Population Grid (GHS-POP)	6
2.1.4 Geospatial Development Mask	6
2.1.5 Administrative Boundaries	7
2.1.6 Degree of Urbanization	7
2.2 Methods	8
2.2.1 Characterizing the model	8
2.2.2 World Regions	9
2.2.3 Gridded Global Spatial Population Scenarios	9
2.2.4 National-Level Built-up Area Change	12
2.2.5 Gridded Global Built-up Area Grids	13
2.2.6 Calibration Results	14
2.2.7. Spatial Population Variants	15
2.2.8. Built-up Land Variants	16
3 RESULTS	17
3.1 Nigeria	18
3.2 Germany	30
4. DELIVERABLES	38
5. REFERENCES	39
ANNEX A: COUNTRIES AND TERRITORIES	41
ANNEX B: DATA DESCRIPTIONS	48
Population Projections	48
Built-up Land Projections	49

1 Background and objectives

Understanding how the spatial distribution of the human population, and corresponding urban development, evolve over time is critical to a variety of planning and policy matters including migration, economic development, and environmental change. Spatial population distributions and urban development are key factors in, for example, land-use and land-cover change [1, 2], habitat and biodiversity loss [3], demands for energy [4], food [5], water [6, 7], spatial patterns of pollutant emissions [8, 9], and the spread of infectious disease [10]. However, to-date there are very few existing global-scale spatially explicit projections of future population and urban development at high resolution. Furthermore, analysis across both large geographic regions and at the local scale suffer from the lack of a globally consistent urban definition, rendering comparative research difficult and regional/local decision-making contentious because key funding resources are often tied to urban status. To meet the needs of many research and planning communities there has been recent progress in the development and application of new methods for constructing scenario-based spatial population projections [11-13]. Advancements in remote-sensing based classification and creation of global land cover and land use data products substantially enhance this process, and for the first time offer opportunities to jointly project changes to both the human and the built environment.

In this work, we apply new methods to project scenario-based, plausible future spatial distributions of the human population and built-up land in support of the European Commission's stated goal: the development of a global, people-based definition of cities and settlements. The methods build on recent research regarding spatial population dynamics and urban spatial development, in large-part rooted in the global change research community. More specifically, we apply a gravity-based downscaling model developed specifically to construct projections that can be calibrated to historic data and parameterized to reflect alternative qualitative assumptions regarding future development pathways [12]. This model is enhanced to consider the symbiotic relationship between spatial population change and changes in the built environment. This report provides technical details of the modelling approach applied to produce the population and built-up land scenarios delivered in fulfilment of the above referenced contract. Section 2 introduces the data used in the modelling, and describes the methodology. Section 3 details the final deliverables, Section 4 provides a discussion of key results and interesting findings, while Section 5 aims to contextualize this work within the current research and discusses expected impacts. Finally, Section 6 reviews potential research directions based on the results and lessons learned of this work.

1.1 Development of new spatial data products

The primary result of this work is the development of two new data products; global-scale population scenarios at 1km resolution for the period 2020-2100 in ten-year intervals, and corresponding global-scale scenarios of built-up land at the same spatial and temporal resolution. Table 1 summarizes the data products.

Table 1. Output data specifications.

Spatial Product	Coverage	Model Application	Resolution		Projection Period	Base-year	Scenario	Units
			Spatial	Temporal				
Population	Global	National	1km	10 year	2020-2050	2015 GHS-Pop	SSP 2 & variants	Count of persons
Built-up land	Global	National	1km	10 year	2020-2050	2014 GHSL	SSP 2 & variants	Portion (%) of grid cell built-up

The spatial population data are produced by downscaling national-level aggregate projections drawn from the Shared Socio-economic Pathways (SSPs; [14]) to 1km grid-cells. The downscaling model developed for this work is applied at the national-level for 240 countries and territories to produce global coverage (see Annex A for complete list). The spatial population data are provided as gridded layers stored in geodatabases, by world region (Figure 2), for each 10-year time step. Each 1km grid cell contains a count of the number of persons projected to reside within that cell at each point in time. In total, we produce four scenarios based on SSP2 (middle-of-the-road scenario). The primary SSP2 scenario (SSP2 hereafter) assumes a spatial pattern of population change for each country consistent with observed trends over the period 1990-2015. The remaining three scenarios are each variants of SSP2, in which patterns of spatial population change reflect convergence towards a specific style of urbanization; high, medium, and low density (high, medium, and low variants hereafter; discussed in more detail below). The starting point for these scenarios is the observed spatial distribution of the population in 2015 at a resolution of 1 km, as characterized by 2015 GHS-Pop data [15].

The 1km gridded built-up land data are also produced using a downscaling model. However, an important distinction between the spatial population and built-up land scenarios is that while the aggregate national-level population data used as inputs to the downscaling model are available as part of the existing SSPs developed by the global-change community, corresponding built-up land scenarios are not. Thus, for this work we developed new built-up land projections at the national-level, for SSP2 and each variant, for each of the 240 countries and territories that comprise global coverage using the same 10-year time steps. For SSP2, the projection is created by assuming the historic relationship between national-level population change and built-up land change in the past decades remains constant moving into the future (an assumption consistent with the business-as-usual nature of SSP2; this process is discussed in more detail in section 2.2.4). Similarly, for each of the variants, convergence towards a specific style of development is assumed, in this case reflected by the built-up per capita ratio corresponding to the high, medium, and low density patterns of spatial population change. The spatial built-up land layers represent, at 1km resolution for each 10-year period, the portion of each grid cell that has been developed (i.e., through man-made structures or buildings). The starting point for these scenarios is the observed spatial distribution of the built-up land in 2014 at 1km resolution as characterized by the 2014 GHSL data [16]. The process of developing each of these data products is discussed in full detail in Section 2.

2 Data and Methods

2.1 Input data

Table 2. Input data for population and built-up area models.

National population projections	Shared Socioeconomic Pathways (SSPs)	IIASA	SSP2	National	2010-2100; 5-year
	World Population Prospects - 2019 Revision*	UN Population Division	Medium Variant	National	2020-2100; 1-year
Population Distribution	Global Human Settlement - Population (GHS-Pop)	JRC-EC	n/a	1km	1990, 2000, 2014
Built-up land	Global Human Settlement Layer (GHSL)	JRC-EC	n/a	1km	1990, 2000, 2015
Elevation/Slope**	Shuttle Radar Topography Mission (SRTM)	USGS	n/a	90m	2018
	Global Multi-Resolution Terrain Elevation Data (GMTED)***	USGS	n/a	250m	2018
Surface Water**	World Water Bodies	ESRI	n/a	Vector	2018
Protected Land**	World Data on Protected Areas (WDPA)	IUCN	n/a	Vector	2019
Administrative Boundaries	Global Administrative Areas (GADM) v2.8	GADM	n/a	1km****	2018

* Used only for countries and territories not specifically included in the SSPs

** Input to the Geospatial Development Mask

*** GMTED is used in place of SRTM above 60°N Latitude, an area for which there are no SRTM data

**** The native GADM data are vector format, but are transformed into a 1km raster with each grid cell assigned to only one country

2.1.1 National-level population scenarios: The shared socioeconomic pathways

The five SSPs span a wide range of possible future development pathways and describe trends in demographics, human development, economy and lifestyle, policies and institutions, technology, and environment and natural resources. Trends are described for three broad country groups from the present through the end of the century. For most demographic factors, those groups are the currently high fertility countries, low fertility countries with high incomes (i.e., in the OECD), and other low fertility countries. For assumptions about urbanization levels, country groups are somewhat different, defined by current income levels alone.

In this work we only consider SSP2 (as the “middle of the road” scenario), which describes a world with development that occurs at rates consistent with historical patterns, and therefore has moderate levels of investment in human capital, technological change, and economic growth. Demographic outcomes are consistent with middle of the road expectations about population growth, urbanization, and spatial patterns of development. Trends vary across regions and over time, but on average fall near the centre of expectations about future outcomes rather than toward the upper or lower bounds of possibilities. Global population peaks at about 9.5 billion in 2070, then declines to just under nine billion by the end of the century. The global urbanization rates continue to rise steadily, hitting 66% by mid-century and reaching 80% by 2100. National-level population projections for SSP2 were produced by the International Institute for Applied Systems Analysis (IIASA) and can be downloaded through the SSP Database (<https://tntcat.iiasa.ac.at/SspDb/dsd?Action=htmlpage&page=about>).

Some very small countries and autonomous territories are not included in the SSP-database. When missing, we supplemented the national-level projections with the medium variant projections from the 2019 Revision of the United Nations World Population Prospects. A full list of countries and territories independently modelled in this work can be found in Annex A.

2.1.2 The Global Human Settlement Layer (GHSL)

The Global Human Settlement Layer, produced by the Joint Research Centre (JRC) of the European Commission, is a remote sensing-derived global data product that represents built-up land for different points in time over 40 years (1975, 1990, 2000, and 2014) at fine spatial resolution (approximately 38 meters, aggregated to 250 meters). The original resolution data are binary, indicating either the presence or absence of a built structure intersecting with a 38m-resolution grid cell [16-18]. The aggregated data are constructed from the 38m cells to quantify the percentage of each cell that is built-up. This construction implies an aggregation of the original data to 304m and a subsequent resampling step to 250m to facilitate compatibility with other 1 kilometre global land cover and population data products. A recent validation study has generally confirmed acceptable levels of accuracy of the GHSL data layers for different points in time in urbanized settings but also reported higher levels of classification errors in rural regions (for details see [19]).

2.1.3 The Global Human Settlement Population Grid (GHS-POP)

GHS-POP [20] is a medium-resolution spatial raster dataset that depicts the distribution and density of population, expressed as the number of people per cell at 250m and 1km resolution for 1975, 1990, 2000, and 2015. To derive residential population estimates for each time period, population data from national censuses or administrative units, provided by CIESIN GPWv4, were disaggregated and reallocated to grid cells. The process was guided by the distribution and density of built-up area as indicated by the GHSL global layer for each time period.

2.1.4 Geospatial Development Mask

To better project future change in the spatial distribution of the population and built-up land, we use the geospatial development mask developed for spatial projections of the existing five SSPs [12]. The index, constructed from four geospatial layers, precludes land from development (e.g., human settlement) as a function of; (1) elevation, (2) slope, (3) surface water, and (4) mandate for protection. The term itself ranges from 0 to 1 and indicates the portion of each grid cell that is suitable for human habitation, as is illustrated in Figure 1. The ESRI World Water Bodies [21] dataset is used to mask global surface water. Elevation and slope data are from the Global Multi-resolution Terrain Elevation Data 2010 (GMTED2010) [22]. The elevation of the highest permanently populated settlement in each continent denotes a ceiling to exclude land from future habitation as a function of high elevation. In general, development costs increase substantially on land exhibiting a slope greater than 15%, which is also the point at which many municipalities impose development regulations [23]. The index accounts for the likelihood that improved technology will reduce the costs associated with excess slope, and instead impose a threshold of 25%, an oft-cited “no-development” threshold in municipal regulations across the United States [e.g., 24]. Finally, the International Union for the Conservation of Nature (IUCN) World Database on Protected Areas (WDPA) is used to mask land as a function of mandate for protection [25]. Specifically, any area classified under IUCN categories Ia (strict nature reserve), Ib (wilderness area), II (national park), III (national monument or feature), or IV (habitat/species management area) is masked as not suitable for development/ habitation.

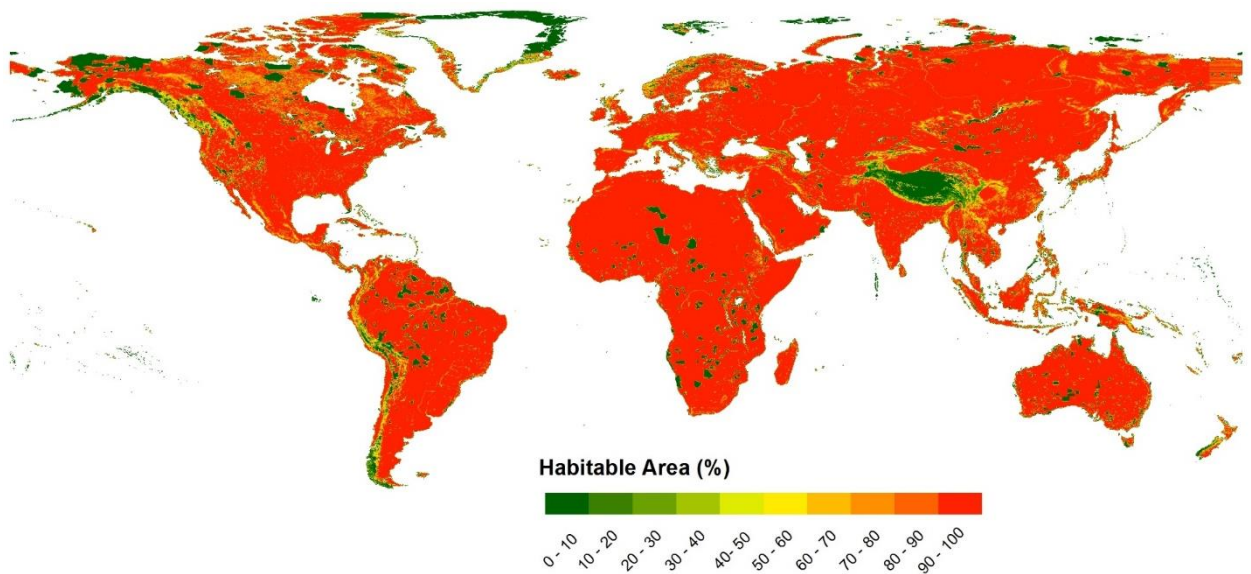


Figure 1. Habitable land by grid cell after application of the geospatial mask.

2.1.5 Administrative Boundaries

National and territorial boundaries are taken from the Global Administrative Areas database (version 2.8). The data are compiled by a consortium of scientists and are made publically available for use in GIS and programming applications. They are widely purported to represent the highest resolution administrative units available for each country. In their native format the data are vector polygons, however here we use the raster version in which each 1km grid cell is assigned to only one country (eliminating any boundary overlap) using a majority rule.

2.1.6 Degree of Urbanization

In its 51st session (March 2020; [26]), the United Nations Statistical Commission endorsed a new methodology for delineation of cities and urban and rural areas for international and regional statistical comparison purposes. The method was proposed by a consortium of six international organizations led by the European Union (EU), and including the Food and Agriculture Organization of the United Nations (FAO), the International Labour Office (ILO), the Organization for Economic Co-operation and Development (OECD), United Nations Human Settlements Programme (UN-Habitat) and the World Bank. This was launched at the Habitat III conference in 2016.

The goal of the method is to facilitate international statistical comparisons of cities, urban, and rural areas, across a selection of indicators, and is meant to complement rather than replace the definitions used by national statistical institutes and ministries. These national definitions typically rely on a much wider set of often disparate indicators, rendering meaningful comparison difficult [27].

The method, called the Degree of Urbanization, classifies the entire territory of a country into three classes: 1) cities, 2) towns and semi-dense areas and 3) rural areas, which are further divided in an extension of the approach into cities, towns, suburban or peri-urban areas, villages, dispersed rural areas, and mostly uninhabited areas. The method is meant to better capture the urban-rural continuum, because it is

based on a population grid, it reduces the distortions created by the variable size of statistical and administrative units [27].

2.2 Methods

In this section, we introduce and detail the methods we apply to complete the assignments as described in the technical specifications. The population and built-up land models are introduced separately, however each informs the other to a certain degree. That is to say, the proposed framework is such that population and built-up land evolve, in part, as a function of the initial conditions of one another, and yet are independent to the point that the spatial relationship between them will shift over time. For both the population and built-up grids, we projected from 2010 to 2100 in 10-year intervals over a global 1 km² grid. Base-year data were the 2015 GHS-POP and the 2014 GHSL layer (built-up). To calibrate our models we used the historic GHS-Pop and GHSL for the periods, 1990 and 2000 in conjunction with the 2015 data. Models were applied at the national-level and include 240 countries and territories included in the SSP-based projections from Jones and O'Neill [12] which comprises an exhaustive list of the administrative units for which either IIASA or the United Nations produces future population projections. As previously noted, we produce a primary SSP2 scenario that assumes a continuation of regional trends in spatial population and built-up land change. Additionally, we produce three variants of SSP2 assuming convergence towards high, medium, and low density urbanization. The population and built-up models are described as applied to the SSP2 scenario in Sections 2.2.3 -2.2.5 below. To produce the variants we make minor adjustments to the methods, inputs, and specifications. Details regarding the variants are presented in Sections 2.2.7 and 2.2.8.

2.2.1 Characterizing the model

The model is a form of gravity-based spatial allocation approach applied over a continuous raster surface (e.g., subnational 1km grid cells comprising all land area in any given country) that bears similarities with many types of dasymetric mapping. Gravity-type approaches are commonly used in geographic models of spatial allocation and accessibility. They take advantage of spatial regularities in the relationship between population agglomeration and spatial patterns of population change. These relationships can be described as a function of the characteristics known to correlate with spatial patterns of population change. The model uses a modified form of population potential, a distance-weighted measure of the population taken at any point in space that represents the relative accessibility of that point (for example, higher values indicate a point more easily accessible by a larger number of people). Population potential can be interpreted as a measure of the influence that the population at one point in space exerts on another point. Summed over all points within an area, population potential represents an index of the relative influence that the population at a point within a region exerts on each point within that region, and can be considered an indicator of the potential for interaction between the population at a given point in space and all other populations [28]. This potential will be higher at points closer to large populations; potential is thus also an indicator of the relative proximity of the existing population to each point within an area [29]. Such metrics are often used as a proxy for attractiveness, under the assumption that agglomeration is indicative of the various socioeconomic, geographic, political, and physical characteristics that make a place attractive.

For purposes of drawing appropriate conclusions from the results, it is important to note the strengths and weaknesses of the approach, and more simply, what the model

does and does not do. Gravity-type models are particular well-suited to capturing and modelling broad trends in spatial data. As such, this approach will allow the user to specify a model that will replicate commonly observed patterns such as dispersion or concentration. Additionally, added complexity will allow for some assessment of local deviation from broad trends through examination of covariates. However, here we are only considering the influence of population and built-infrastructure on one another as evidenced by their co-variance over time. More simply, we are taking advantage of observed regularities in the co-evolution in population and built-up land to project both into the future. As such, this model does not allow us to specifically comment on the drivers of population and/or built-up land change. Instead, we are using the empirical record to project what the future world might look like if observed spatially explicit mathematical regularities continue. Future work could extend this (or another similar) approach to better assess the drivers of change in population and the built-environment.

2.2.2 World Regions

Because the GHS-POP data are constructed using the Gridded Population of the World version 4 (GPWv4; [30]), we cannot calibrate the population model for every country (as not all of the time series data from GPWv4 are based on consecutive censuses but instead in countries for which only one census period was available as inputs, are scaled versions of the same census). The population model requires data from two consecutive census periods to ensure that parameter estimates are indicative of actual patterns of spatial change. To address this problem we divide the world into 20 regions, and for each regions select marker counties for which adequate historic data exist to estimate parameters (in many cases this will be more than one country). For countries with inadequate historic data, we will apply parameters estimated from the regional marker country. World regions are illustrated in Figure 2, and are based on existing UN definitions.

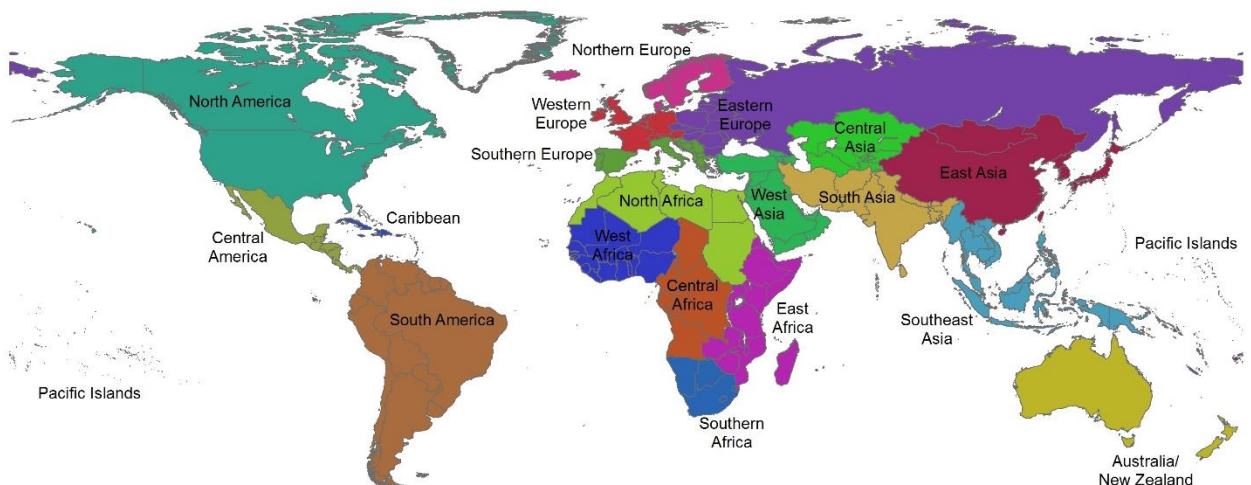


Figure 2. World regions.

2.2.3 Gridded Global Spatial Population Scenarios

The spatial population downscaling model is based on the INCLUDE model, developed to produce spatially explicit population scenarios for the global change research

community [11, 12]. Several changes to the algorithm are adopted to better facilitate the goals of this work, the most notable of which are (1) treating urban and rural populations together¹ and (2) identifying and modelling the relationship between built-up and land and population change over space. The SSPs include national-level projections of change in the urban and rural population components of the total population. However, adhering to the prescribed urbanization scenario and downscaling population as a function of its components would have the effect of exogenously controlling the size of cities rather than allowing them to evolve endogenously. Because a primary goal of this work is the application of the newly developed Degree of Urbanization algorithm, the decision was taken to project scenarios under population change as described by SSP2, absent the urbanization rate. As such, outcomes from this model may deviate from the urbanization rate prescribed by the SSPs, subject to the definition of “urban” that is applied. The second major change was introducing the built-up nature of the landscape as a potential driver of future spatial population change. Practically, this means the presence of infrastructure acts as a potential pull-factor for future local population growth, while the absence of building infrastructure has the opposite impact. The full procedure is now discussed in further detail.

Beginning with a gridded distribution of the base-year (2015) population the model iterates two procedures for each 10-year time-step: (1) calculate a subnational population potential surface (a distribution of values reflecting the relative attractiveness of each grid cell), and (2) allocate projected national-level population change to grid-cells proportionally according to their respective potentials. Grid cells may gain or lose population at any time step as a function of their relative attractiveness (or repulsiveness) regardless of the general trend (e.g., national-level growth or decline). From a technical standpoint, this can occur because both positive and negative potential values are possible at any given location at any given point in time.

Potential for each cell is calculated as:

$$v_{i,t} = l_i \left[\left(\sum_{j \neq i}^m P_{j,t} e^{-\beta d_{ij}} \right) + \alpha_i P_{i,t} \right] \quad (1)$$

where $v_{i,t}$ is potential of cell i at time t , l_i is a geospatial mask indicating the portion of each cell that is suitable for human habitation (see section 2.1.4), $P_{j,t}$ is the population of grid cell j , d is geographic distance between two grid cells, α and β are the population and distance-decay parameters, respectively, and j is an index of the m cells within a 30 km window² around cell i . The β parameter (distance-decay) is

¹ Previous iterations of the model considered urban and rural populations as separate but interacting components of the total population because the historic data indicate that urban and rural people exhibit very different patterns of spatial population change [11]. It is important to note that here the terms “urban” and “rural” refer to people as opposed to urban land, with the former representative of persons leading an “urban lifestyle”. Such households typically interact with cities or larger settlements on a daily basis as a function of employment, economic activities, social and educational opportunities, etc. Urban people usually live in close proximity to, or in cities and large settlements, but they *do not* always live on land that qualifies as “urban” or “built-up”. We have found that the distribution of urban people tends to extend well beyond the boundaries of land-based urban areas (those defined using a built-up area threshold, for example) when using products such as the GHSL in conjunction with census-based urban definitions [31].

² All cells j within 30 km of cell i contribute to the potential of each cell i (the “model bandwidth”). Previous versions of this model considered wider bandwidths of up to 100km [11, 12], a distance derived using the United States Household Transportation Survey and thus specific to the US. Because Americans are not representative of the wider world in terms of travel habits the bandwidth has been modified to reflect a more realistic “sphere of influence”

indicative of the shape of the distance-density gradient controlling the broad pattern of horizontal/vertical development. The α parameter (population) is indicative of the degree to which characteristics of the built environment (here GHSL built-up) lead to proportionally larger or smaller gains/losses in population. Thus, the α parameter weights up or down the contribution of each cell's own population to its potential. Thus, the relative attractiveness of each location is modelled as a function of its population, characteristics of the local built environment, and the agglomeration effect. The latter, recalling from section 2.2.1, is theorized to correlate strongly with the various socio-economic characteristics of places that attract or repel population (unemployment, average income, sectoral employment structure, education, etc.).

In order to carry out steps 1 and 2 we must produce estimates of the α and β parameters by fitting the model to historic data, requiring spatial population data from at least two consecutive periods (e.g., GHS-POP 2000 and 2015). To do so we will use two separate procedures. The β parameter is designed to capture broad-scale patterns of change found in the distance-density gradient (see Figure 3). The negative exponential function in Equation 1 is very similar to Clark's [32] negative exponential function that has been shown to accurately capture observed density gradients throughout the world [33]. The Clark formulation includes a single distance-decay parameter that can be extracted by fitting the function to observed spatial data. To estimate β we will employ a similar technique, and fit the model in Equation 1 to historic population change data (e.g. GPW 1990, 2000, 2010). For purposes of estimating β we will hold α constant at 1 (the value it would assume in the Clark formulation) and adjust the value of β such that we minimize error:

$$S(\beta) = \sum_{i=1}^n |P_{i,t}^{mod} - P_{i,t}^{obs}| \quad (2)$$

where $P_{i,t}^{mod}$ and $P_{i,t}^{obs}$ are the modelled and observed populations in cell i , and S is the sum of absolute error across all cells.

In this modified version of the model the α parameter is a cell-specific measure that is indicative of the impact of the local built-environment on spatial population change. To estimate the parameter for each grid cell we first use the value of β from Equation 2 to generate a projected population field (still holding α constant at 1). The gradient of spatial change in this projection will be relatively smooth (see "Projected" in Figure 3). For each cell, there will be an error in the projected population (the difference between the observed and projected populations in Figure 3). For this work, we use the GHSL built-up value (characteristics of the built environment) an explanatory variable. To incorporate the effects, we calculate the value of α necessary to eliminate the error (from Equation 2) for each individual cell:

$$\Delta P_{i,t}^{obs} = \alpha_i * \Delta P_{i,t}^{mod} \quad (3)$$

where $\Delta P_{i,t}^{obs}$ and $\Delta P_{i,t}^{mod}$ are the observed and modelled population change for each cell i and α_i is the factor necessary to equate the two. The second step is to estimate the relationship between observed index α_i and cell-specific characteristics by fitting a spatial lag model:

$$\alpha_{i,t} = \rho W \alpha_{i,t} + \beta_1 GHSL_{i,t} + \varepsilon_{i,t} \quad (4)$$

of the average global citizen (e.g. the area in which the average person carries out his/her daily business). Additionally, because the contribution of cells beyond 40-50km to the potential of any given cell i is negligible in most cases, a narrower bandwidth is not only more realistic, but facilitates reduced computational time.

where $GHSI_{i,t}$ is the portion of each 1km grid-cell i that is built-up at time t , ρ is the spatial autocorrelation coefficient, and W is a spatial weight matrix. From this procedure, a set of cell specific α values are estimated.

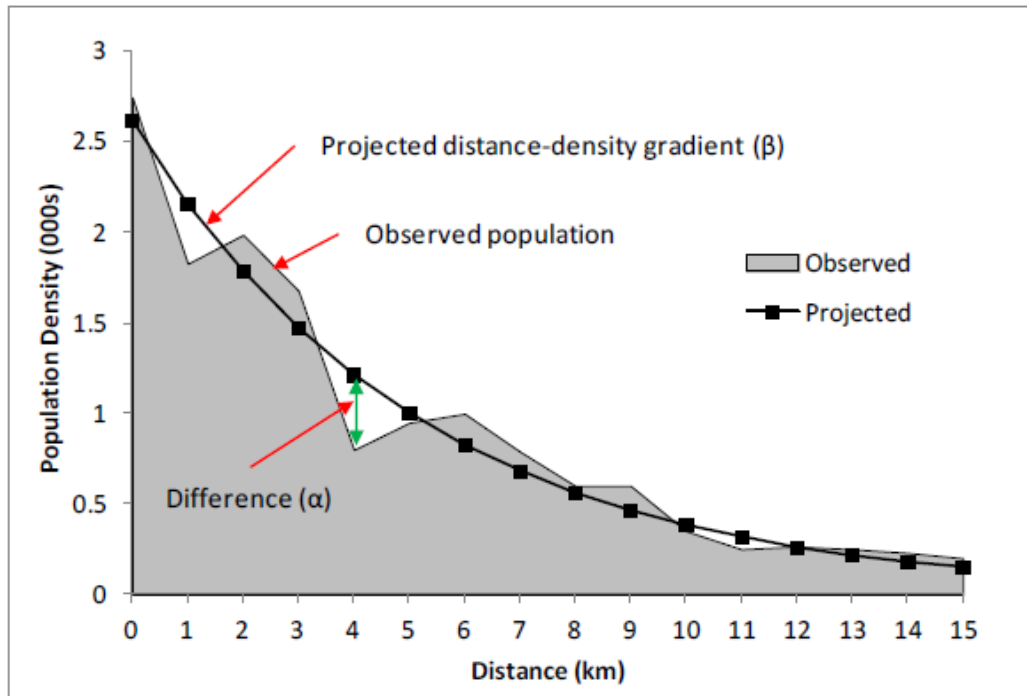


Figure 3. Envisioning the α and β parameters in the context of a stylized distance-density gradient.

For future projections, we use the value of $GHSI_{i,t}$ in 2015 to estimate cell-specific values of $\alpha_{i,t}$. As such, the gravitational “pull” of each grid cell will vary as a function of its current population, its built infrastructure, and the distance weighted population in nearby cells (the neighbourhood effect). Finally, to produce a spatially explicit population projection for SSP2 we use our estimates of α and β and exogenous projections of national population change and apply the model as specified in Equation 1.

2.2.4 National-Level Built-up Area Change

To facilitate the co-production of change in the built-environment we developed a set of national-level “demand for built-up land” scenarios that correspond to the national-level population projections from SSP2. To do so, we adopted a two-phased approach. First, for each country we fit a linear model to the historic GHS-Pop and GHSI data for the period 1990-2015 to estimate a simple model describing change in built-up land as a function of population change. The coefficients on built-up land were catalogued according to country and region (see Figure 2 above). Second, to project aggregate change in built-up land into the future we apply the coefficients generated in the historical analysis along with future population projections to estimate growth in built-up land. However, because the relationship between population and built-up land change varies substantially when aggregate population change is positive or negative, we must consider the directionality of the population projection in each future time step (e.g., growth/decline). When the trend in national-level population change in the historic period coincides with that projected into the future (e.g., growth) we apply coefficients generated from the historic data for each

country. When the future trend runs counter to the historic trend (e.g., projected decline, historic growth), we select coefficients from a representative country (in most cases from the same world region) that have been estimated from a historic period reflecting the correct trend in national-level population change.

2.2.5 Gridded Global Built-up Area Grids

We applied a model similar in structure to the gravity-based approach of the spatial population model to produce projections of built-up area change that correspond to the SSP2-based spatial population scenarios. The gravity structure is useful for several reasons. First, as demonstrated in past application of the population model, we can parameterize the model to reflect both broad scale patterns of spatial change as well as local deviation from those patterns. Second, the gravity approach is premised on one of the primary rules of spatial analysis, places that are near to one another tend to be more similar than places further away from one another. This is to say, the gravity model captures the neighbourhood, or agglomeration effect, which in the context of built-up area suggests that land near already built-up land is more likely to be built-up in the future than land that is in close proximity to undeveloped land.

The method, instead of projection a simple yes/no built-up status for each 1km cell, projects the built-up area of each cell as a proportion of the total area, thus rendering the data consistent with the historic GHSL. Logically then, a cap of 100% and floor of 0% are enforced. At each time step, for each grid cell, built-up area was calculated as:

$$y_{i,t} = l_i \left[\left(\sum_{j \neq i}^m B_{j,t} e^{-\beta d_{ij}} \right) + \alpha_i B_{i,t} \right] \quad (5)$$

where $y_{i,t}$ is the potential of cell i at time t , $B_{i,t}$ is the portion built-up of grid cell i at time t , $B_{i,t+1}$ is the portion built up of grid cell i in the subsequent time step, $B_{j,t}$ is the portion built-up of all grid cells j within a given distance m of cell i , l_i is a geospatial mask indicating the portion of each cell that is suitable for development, β is the distance-density parameter, a universal parameter indicating the strength of the neighbourhood or agglomeration effect (the degree to which cells evolve to look like their neighbours), and α is a cell-specific parameter indicating the degree to which local conditions drive the likelihood (or lack thereof) of growth in built-up area. The spatial mask l is identical to that depicted in Figure 1 above as logic follows that land not suitable for human habitation is not suitable for building, and vice-versa.

The model was calibrated in manner similar to spatial population model as well. The universal distance-decay parameter (β) was estimated for each country by fitting the model to historic periods of observed change, holding α constant at 1 and minimizing the sum of squared errors in:

$$S(\beta) = \sum_{i=1}^n (B_{i,t}^{mod} - B_{i,t}^{obs})^2 \quad (6)$$

where $B_{i,t}^{mod}$ and $B_{i,t}^{obs}$ are the modelled and observed proportion built-up in cell i , and S is the sum of squared error across all cells.

The α parameter was calibrated in the manner depicted in Figure 3 above, producing a distribution of built-up based on the distance-decay parameter (β), calculate the cell-specific error in the change in built-up area, as well as the value of α necessary to eliminate the observed error in each cell i :

$$\Delta B_{i,t}^{obs} = \alpha_i * \Delta B_{i,t}^{mod} \quad (7)$$

where $\Delta B_{i,t}^{obs}$ and $\Delta B_{i,t}^{mod}$ are the observed and modelled change in built-up area for each cell i and α_i is the factor necessary to equate the two. We then hypothesized that this error can be explain, in part, by population density. We estimated this relationship by fitting a spatial lag model:

$$\alpha_{i,t} = \rho W \alpha_{i,t} + \beta_1 D_{i,t} + \varepsilon_{i,t} \quad (8)$$

where $D_{i,t}$ is population density in cell i at time t , ρ is the spatial autocorrelation coefficient and W is a spatial weight matrix. From this procedure, a set of cell specific α values was estimated. To produce a spatially explicit built-up projection for SSP2 we used our estimates of α and β and exogenous projections of change in built-up land (Section 2.2.4) and apply the model as specified in Equation 5.

2.2.6 Calibration Results

The universal parameter β is a good relative indicator of the degree to which the historic evolution of population and/or built-up land has tended towards a more dispersed or concentrated distribution. Lower values of β indicate that the “cost” of movement over space is lower, which translates to a tendency towards dispersion in settlements, while higher values indicate the reverse. Table 3 includes values of β estimated by fitting the model to historic patterns of change in population (GHS-Pop) and built-up land (GHSL). Two patterns are evident in the results. First, dispersed settlement patterns are clearly more evident in North America and Australia/New Zealand, while concentration dominates in East and Southeast Asia. European nations fall between the two extremes, with South/West Asia and North Africa tending, relative to other regions towards dispersion and Latin America more towards concentration. Second, values of β are higher for population than built-up land, indicating that the evolution of built-up land is more dispersed than that of the population. This is likely a function of the nature of the data itself any given grid cell can range only from 0-100% built-up, while population counts vary much more substantially.

Table 3. Distance-Decay Parameter Estimates

	<i>β - Friction of Distance</i>			
	Pop Growth	Pop Decline	BU Growth	BU Decline
North America	1.1	1.99	0.95	1.72
AUS/NZ	1.25	2.1	1	1.68
Sub-Saharan Africa	1.4	2.5	1.29	2.3
South Asia	1.42	2.53	1.3	2.32
West Asia	1.45	2.55	1.3	2.29
North Africa	1.48	2.6	1.21	2.13
Central Asia	1.48	2.6	1.21	2.15
North/West Europe	1.5	2.4	1.36	2.18
South/East Europe	1.53	2.52	1.4	2.31
South America	1.6	2.83	1.5	2.65
Central America	1.6	2.83	1.5	2.65
Caribbean	1.6	2.83	1.5	2.65
Pacific	1.62	2.85	1.54	2.7
Southeast Asia	1.65	2.87	1.52	2.67
East Asia	1.72	2.91	1.61	2.73

2.2.7. Spatial Population Variants

To develop high, medium, and low density variants of the SSP2 scenario first required selecting suitable definitions of what constitutes high, medium, and low population density. We chose to designate world regions as archetypical of each style of spatial population development, and to develop convergence scenarios in which all world regions would evolve towards the pattern exemplified by the representative region for each scenario. Two metrics were considered in selecting representative regions; (1) observed population density by settlement type and (2) estimated β coefficient from the calibration process. Population density by settlement type was assessed by applying the degree of urbanization algorithm to the observed 2015 population distribution, and calculating the population density across each class (primary emphasis was on the urban centres, dense urban clusters, and semi-dense urban clusters classes). We found substantial correlation between population density by degree of urbanization and the estimated value of the β coefficient, with higher density corresponding to higher values of β (see Table 4). As such, we selected East Asia, North/West Europe, and North America as representative of the high, medium, and low density patterns of urban development, respectively.

Table 4. Population density by urban class and friction of distance parameter values in representative regions

Region	Population Density by Urban Class			Distance Parameter	
	Suburbs	Towns	Cities	β Growth	β Decline
North America	749.81	909.29	1,678.41	1.10	1.99
NW Europe	765.42	1,271.81	3,755.58	1.50	2.40
East Asia	908.42	5,328.04	14,965.28	1.72	2.91

For each country, spatial population projections were produced by calculating potential according to Equation 1 and carrying out steps 1 and 2 (section 2.2.3) iteratively, substituting the β parameters from Table 4 that correspond to the representative region for the appropriate variant. Adopting the representative β parameter ensures the appropriate pattern of change occurs within each country for each variant, however further testing revealed that it does not ensure convergence towards the observed population density by urban class (Table 4) representative of high, medium, and low density urbanization. As such, a scaling algorithm was developed for each of the variants and applied to each of the 240 territories and countries to drive population change towards the spatial patterns consistent with each of the variants. The algorithms are designed to scale the population in each grid cell i as a function of the projected population total in that cell (e.g., the scaling factor is a function of the population total itself). The scaling functions, depicted in Figure 4a (2050) and 4b (2100), were derived by fitting a series of functions to the observed data to shift the density in each grid cell towards the “ideal” value observed in each urban class in the representative regions (see “Population Density by Urban Class; Table 4). The process does not immediately shift the population distribution to the pattern apparent in each representative region, but instead drives a shift more slowly over time (reflected in the difference in magnitude of the scaling factors in the 2050 and 2100 functions; Figures 4a relative to 4b). After applying the scaling function, total population was calculated to ensure that application of the function did not change the projected national-level total for each country. If any deviation was found, the

population in each grid cell was then scaled proportional to reconcile the difference. As for the SSP2 projections, the model is applied in ten-year time-steps, however for purposes of assessing the variants (and for deliverables) we focus specifically on 2050 and 2100.

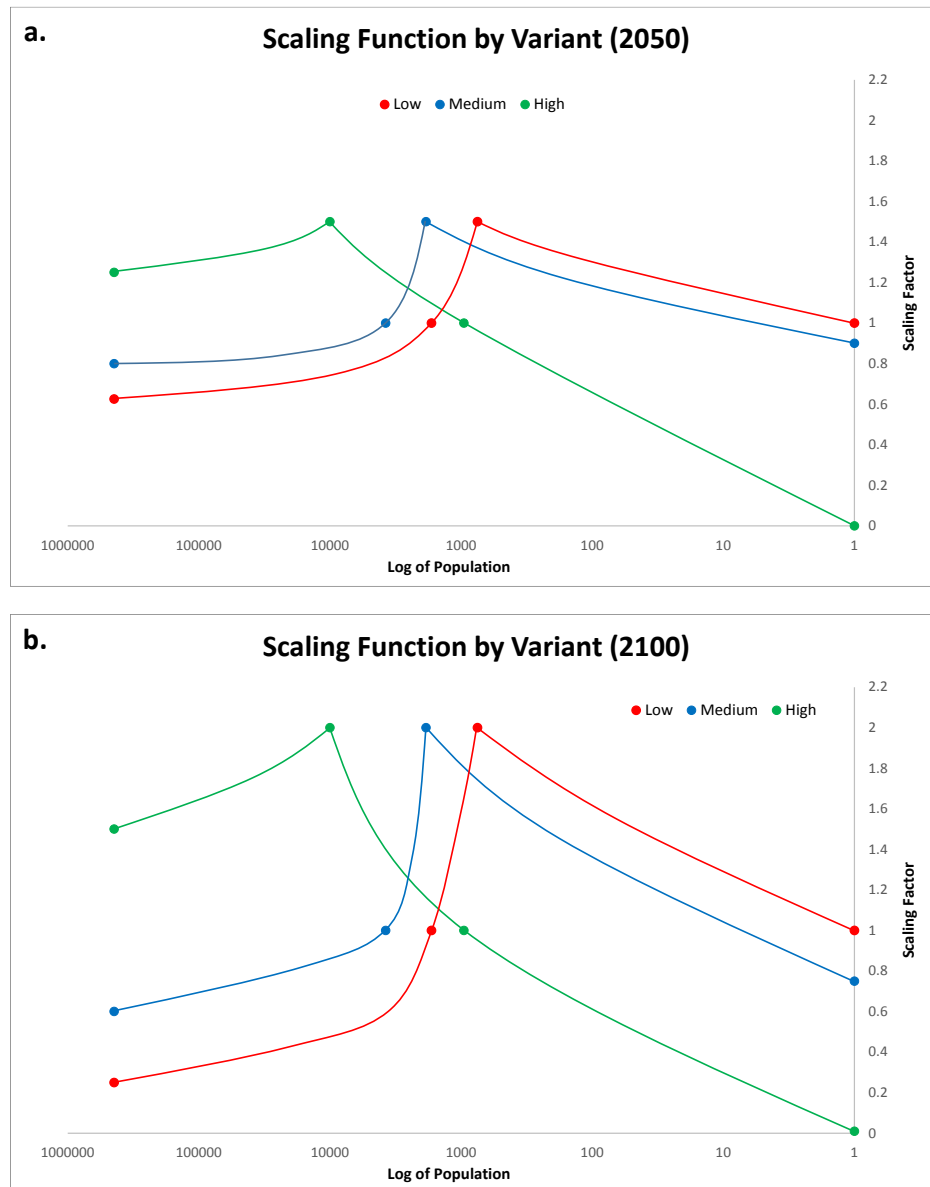


Figure 4. Scaling functions by variant for (a) 2050 and (b) 2100

2.2.8. Built-up Land Variants

The built-up land scenarios for the high, medium, and low density variants of SSP2 are based on convergence towards the pattern of urbanization reflected in the β parameters estimated in the representative regions for built-up land potential (Table 5). Additionally, for each country, a new aggregate estimate of demand for built-up land is derived for each variant by assuming convergence towards the observed level of built-up land per capita from each representative region (Table 5). The built-up

land scenarios for each of the variants are, thus, produced by applying the gravity model as described in Section 2.2.5, substituting the β parameter for each representative region into Equation 5 for the appropriate built-up land scenarios. Built-up land, at each time step, is allocated according to the variant-specific demand for built-up land for each country. If, for any country, convergence towards the observed built-up land per capita of the representative region for any given variant drives demand for built-up land negative, it is assumed that no change in built-up occurs (rather than a loss of built-up land). This occurs, for example, in many countries exhibiting high levels of built-up per capita (e.g., the United States) as they converge towards the high-density pattern of urbanization (e.g., Hong Kong). As with the spatial population variants, the process does not assume an immediate shift to the level of built-up per capita, but instead a slow shift over time. For purposes of the aggregate projections applied here, it was assumed that countries would reach convergence in 2100 (excluding any countries that would require a loss in built-up land to reach convergence – in such cases full convergence is not achieved).

Table 5. Built-up land per capita and friction of distance parameter values in representative regions

Region	Built-up Land Per Capita	Distance Parameter	
		β Growth	β Decline
North America	0.051	0.95	1.72
NW Europe	0.03	1.36	2.18
East Asia	0.0073	1.61	2.73

3 Results

Sample output for the spatial population and built-up land modules are presented here for two countries projected to experience divergent outcomes under SSP2 over the course of the 21st century; Nigeria and Germany. The population of Nigeria is projected to more than triple, from under 200 million in 2015 to nearly 600 million by end-of century. Conversely, the population of Germany, which declined by just over 1 million between 2000 and 2015, is expected to continue slowly declining from roughly 81.5 million in 2020 to just under 80 million by mid-century. The rate of decline is then projected to increase, leaving 66.5 million in the country in 2100. These divergent patterns lead to very different patterns of change in both population and built-up land between the two countries, thus they are illustrative of opposite ends of the development spectrum. Germany is representative of many developed, wealthy nations, while Nigeria is typical of many developing nations. Here, results capture (in tabular and graphic form) the range of outcomes the model is capable of producing for both SSP2 and the variants. Section 3.1 includes results from Nigeria (SSP2 and variants), and Section 3.2 reviews Germany.

3.1 Nigeria

Table 6. Population, land area, and population density by degree of urbanization, SSP2 and variants: Nigeria 2015 and 2050.

	2015						
	Uninhabited Rural	Dispersed Rural	Villages	Suburbs	Towns	Cities	Total
Area	799,355	58,455	14,505	20,004	11,116	13,193	916,628
Pop	647,079	9,058,274	13,768,171	17,858,965	42,641,775	98,167,477	182,141,741
Density	0.81	154.96	949.23	892.77	3836.03	7440.76	198.71

Area	2050						
	Uninhabited Rural	Dispersed Rural	Villages	Suburbs	Towns	Cities	Total
SSP2	748,381	85,505	15,398	32,830	13,222	21,292	916,628
Low	692,718	104,578	15,499	28,031	11,578	64,224	916,628
Medium	748,319	79,115	14,315	24,397	13,472	37,010	916,628
High	851,197	13,980	10,066	11,777	9,576	20,032	916,628

Pop	2050						
	Uninhabited Rural	Dispersed Rural	Villages	Suburbs	Towns	Cities	Total
SSP2	3,105,207	12,523,162	14,930,645	28,817,441	57,190,153	255,128,390	371,694,998
Low	4,532,601	13,904,875	16,282,049	25,224,574	40,639,803	271,111,076	371,694,977
Medium	3,369,515	11,291,788	16,070,801	22,852,161	55,832,547	262,278,194	371,695,007
High	672,212	2,025,562	13,882,749	13,917,638	53,457,211	287,739,645	371,695,017

Density	2050						
	Uninhabited Rural	Dispersed Rural	Villages	Suburbs	Towns	Cities	Total
SSP2	4.15	146.46	969.62	877.78	4325.30	11982.19	405.50
Low	6.54	132.96	1050.52	899.88	3510.09	4221.34	405.50
Medium	4.50	142.73	1122.65	936.68	4144.34	7086.68	405.50
High	0.79	144.89	1379.17	1181.76	5582.42	14364.00	405.50

Table 7. Population, land area, and population density by degree of urbanization, SSP2 and variants: Nigeria 2015 and 2100.

	2015						
	Uninhabited Rural	Dispersed Rural	Villages	Suburbs	Towns	Cities	Total
Area	799,355	58,455	14,505	20,004	11,116	13,193	916,628
Pop	647,079	9,058,274	13,768,171	17,858,965	42,641,775	98,167,477	182,141,741
Density	0.81	154.96	949.23	892.77	3836.03	7440.76	198.71

Area	2100						
	Uninhabited Rural	Dispersed Rural	Villages	Suburbs	Towns	Cities	Total
SSP2	709,467	102,832	15,589	44,876	15,646	28,219	916,628
Low	619,904	37,663	8,278	3,760	3,084	243,939	916,628
Medium	719,420	50,253	12,125	7,827	6,179	120,824	916,628
High	848,800	13,295	10,059	10,071	9,101	25,302	916,628

Pop	2100						
	Uninhabited Rural	Dispersed Rural	Villages	Suburbs	Towns	Cities	Total
SSP2	3,669,940	14,870,415	15,532,142	38,373,747	70,834,467	439,099,315	582,380,026
Low	7,762,808	13,393,931	16,191,551	7,344,080	14,932,116	522,755,520	582,380,006
Medium	5,100,492	11,751,640	22,488,045	12,797,938	35,673,788	494,568,137	582,380,040
High	2,156,418	6,636,365	17,161,637	15,488,879	71,827,268	469,109,462	582,380,029

Density	2100						
	Uninhabited Rural	Dispersed Rural	Villages	Suburbs	Towns	Cities	Total
SSP2	5.17	144.61	996.38	855.11	4527.42	15560.29	635.35
Low	12.52	355.63	1955.97	1953.21	4841.80	2142.98	635.35
Medium	7.09	233.85	1854.68	1635.10	5773.39	4093.29	635.35
High	2.54	499.16	1706.10	1537.97	7892.24	18540.41	635.35

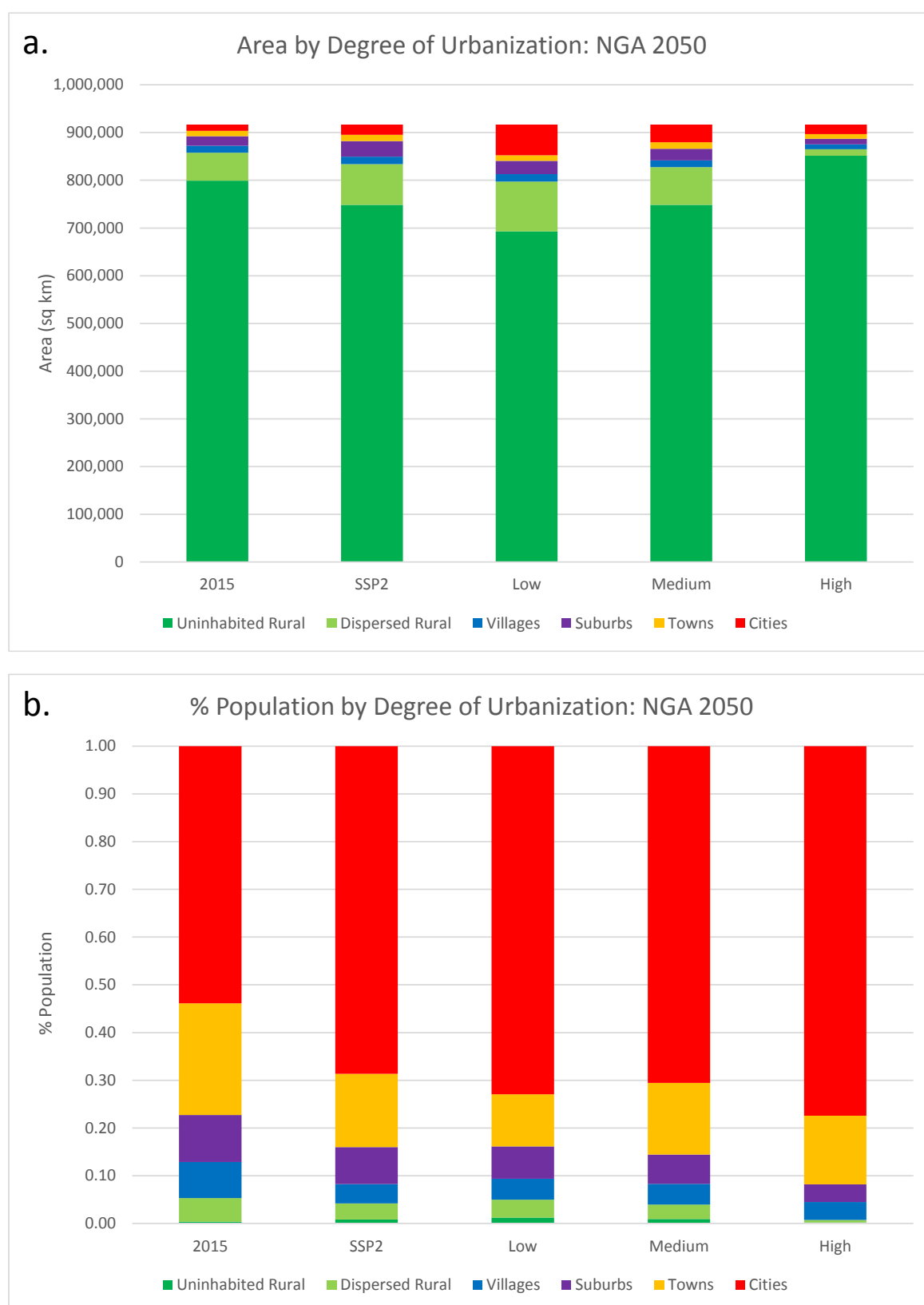


Figure 5. Distribution of (a) land and (b) population by degree of urbanization, SSP2 and variants: Nigeria 2015 and 2050.

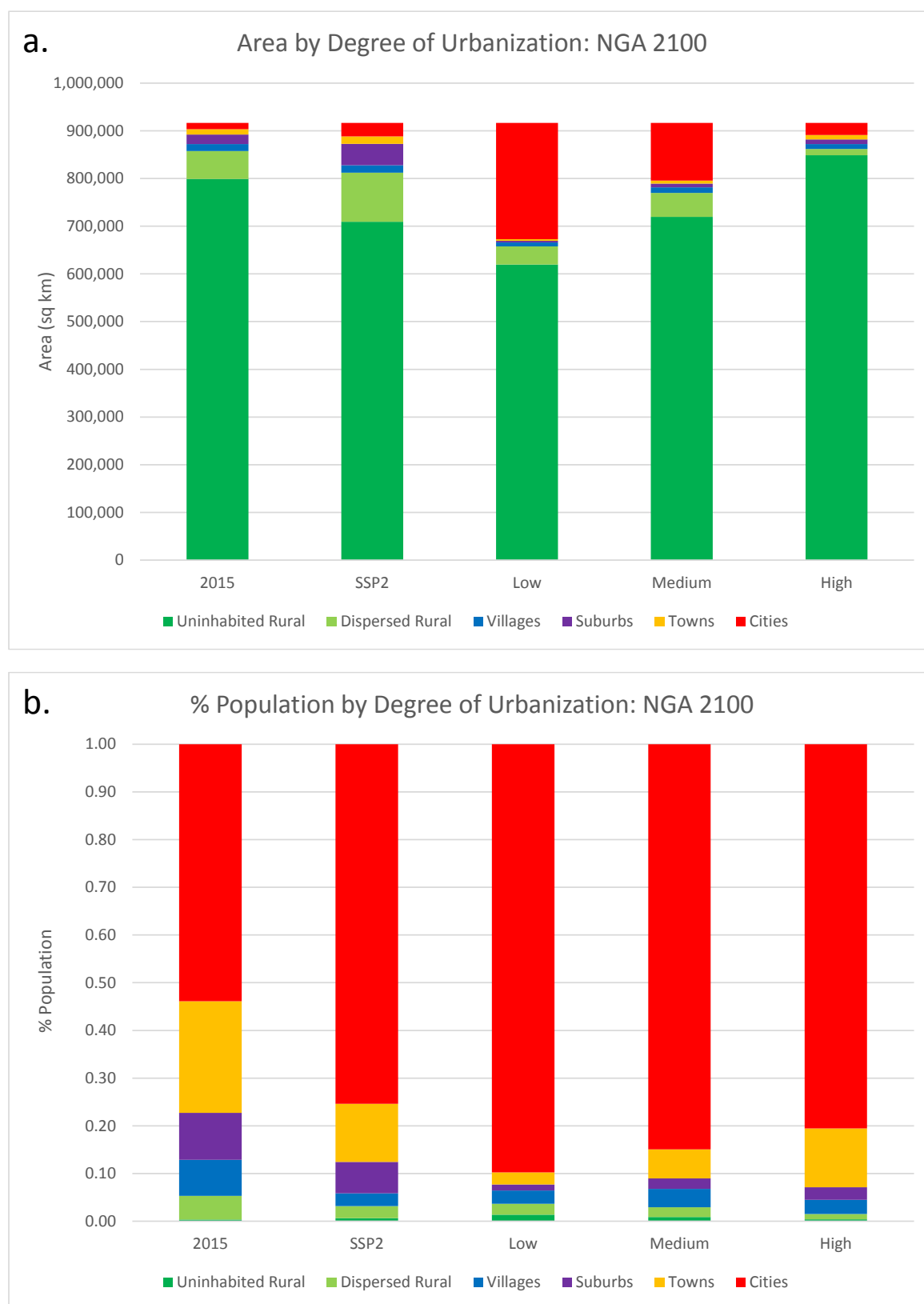


Figure 6. Distribution of (a) land and (b) population by degree of urbanization, SSP2 and variants: Nigeria 2015 and 2100.

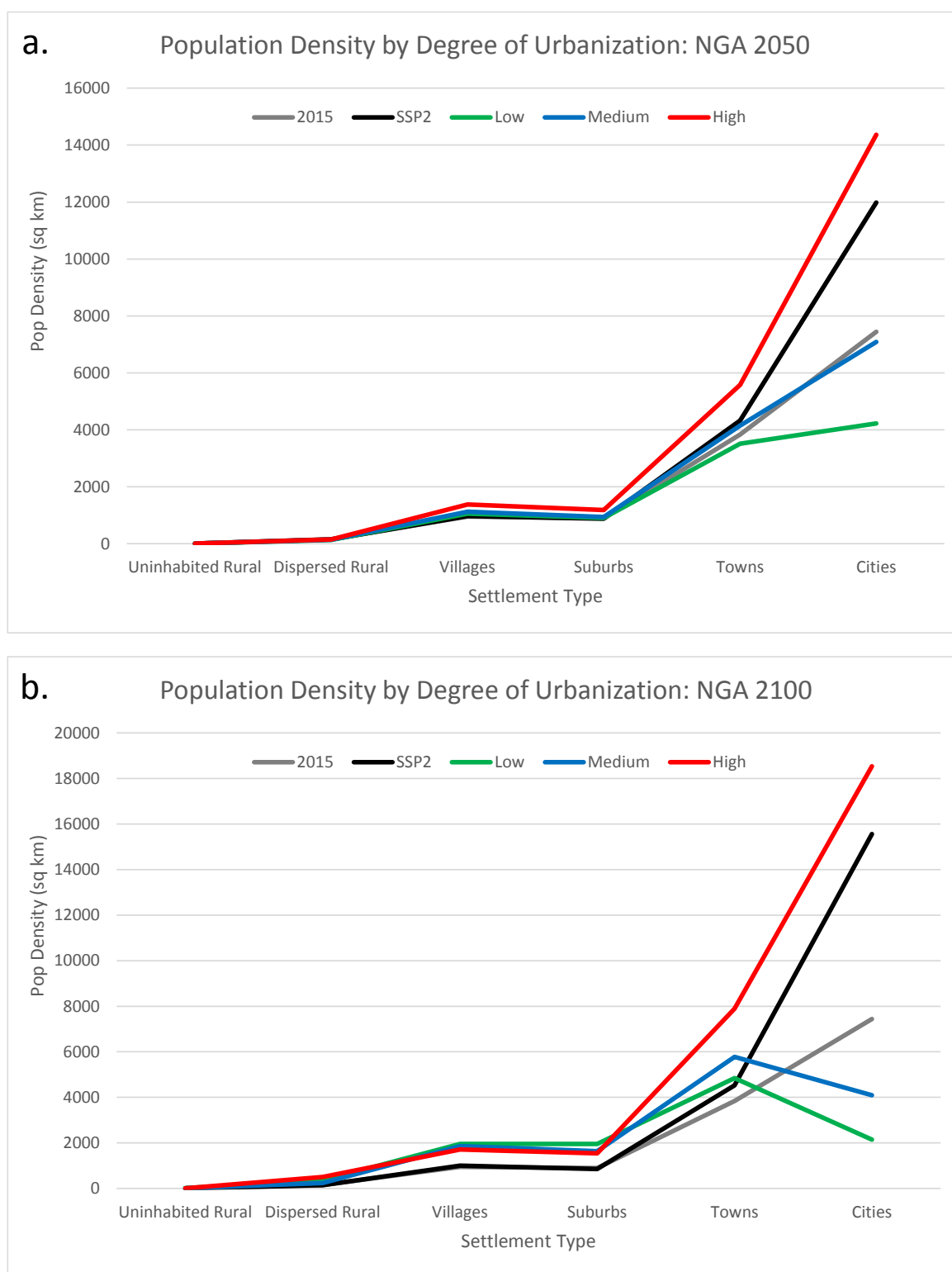


Figure 7. Population density by settlement type for (a) 2015 and 2050 and (b) 2015 and 2100: Nigeria, SSP2 and variants.

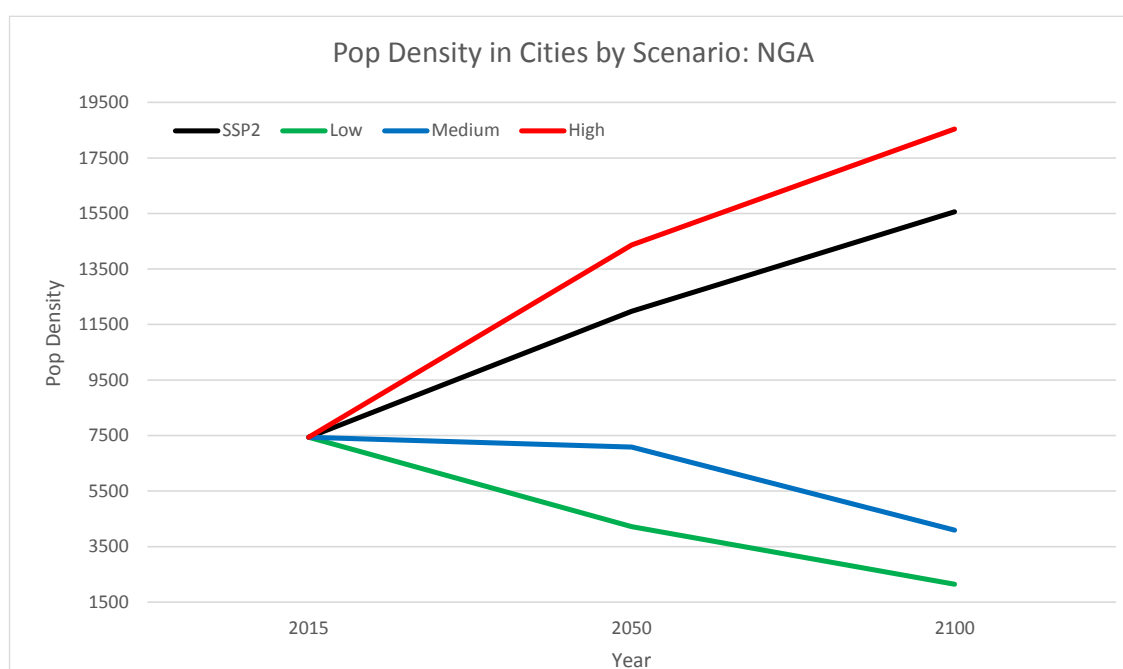


Figure 8. Population density in cities in 2015, 2050, and 2100: Nigeria, SSP2 and variants.

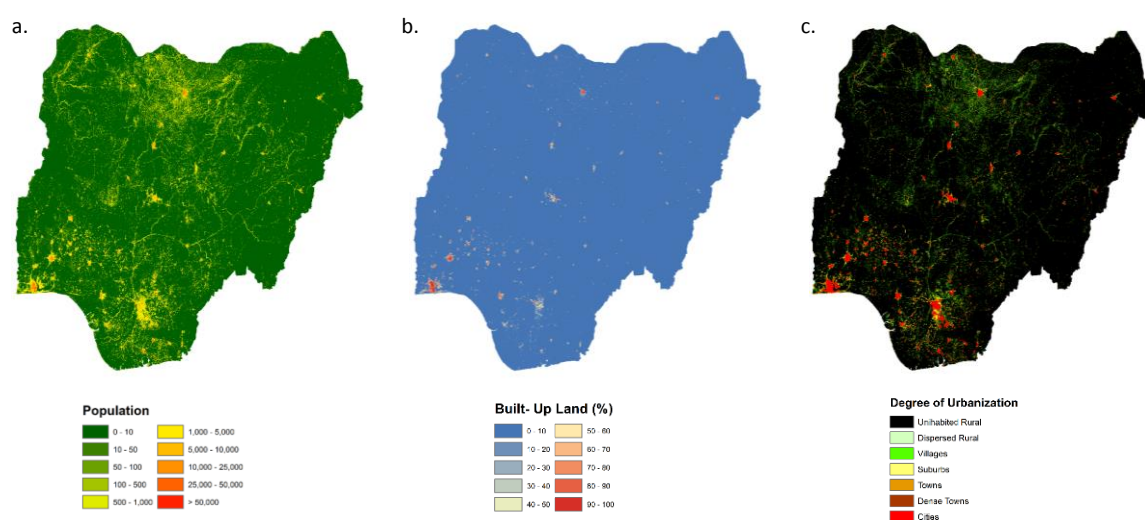


Figure 9. Observed distribution of (a) population, (b) built-up land, and the (c) degree of urbanization; Nigeria 2015.

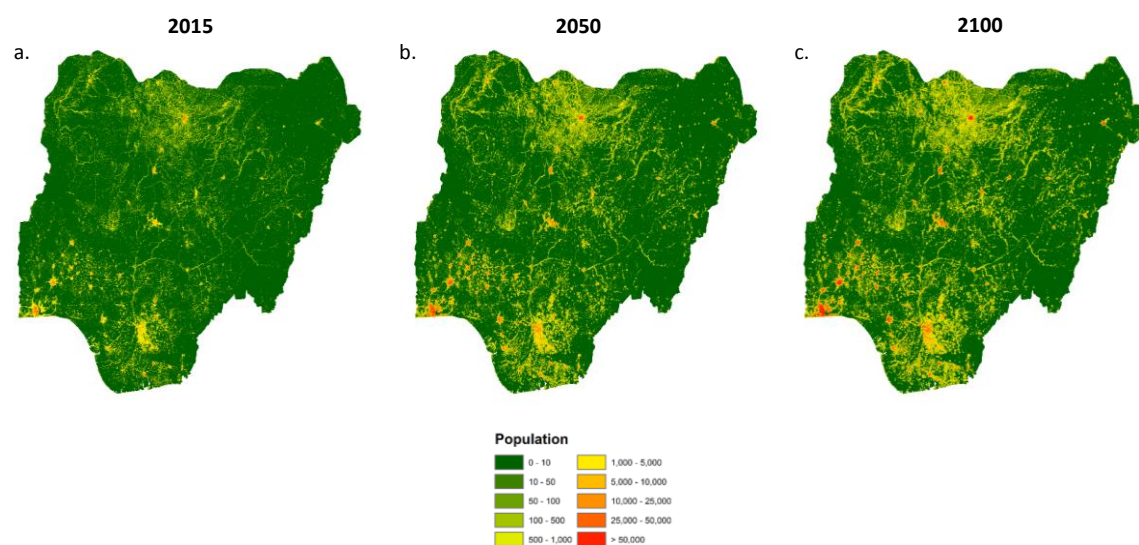


Figure 10. Projected population change, 2050 and 2100: Nigeria SSP2

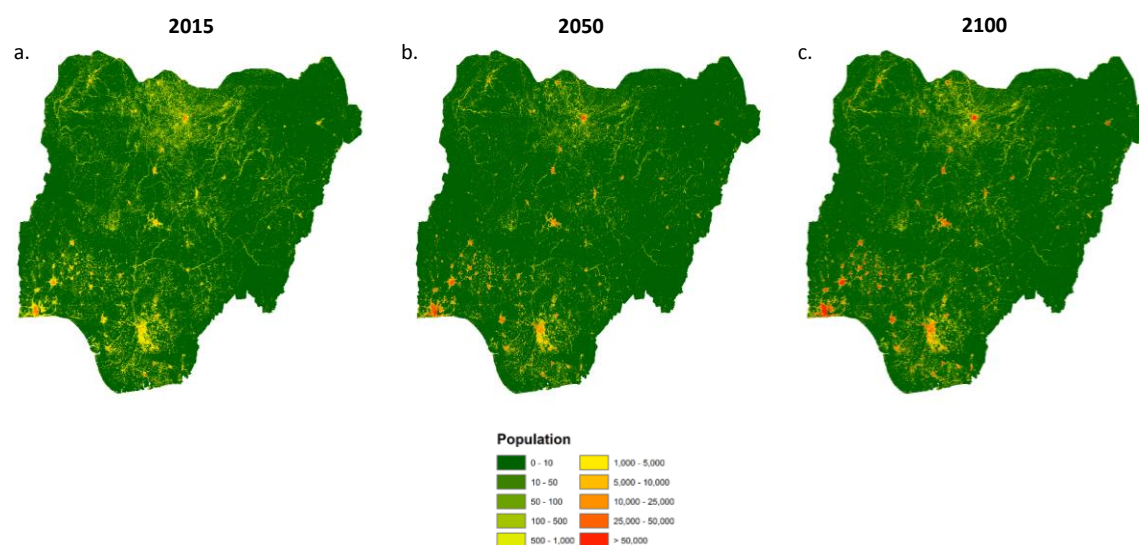


Figure 11. Projected population change, 2050 and 2100: Nigeria SSP2 – High Variant

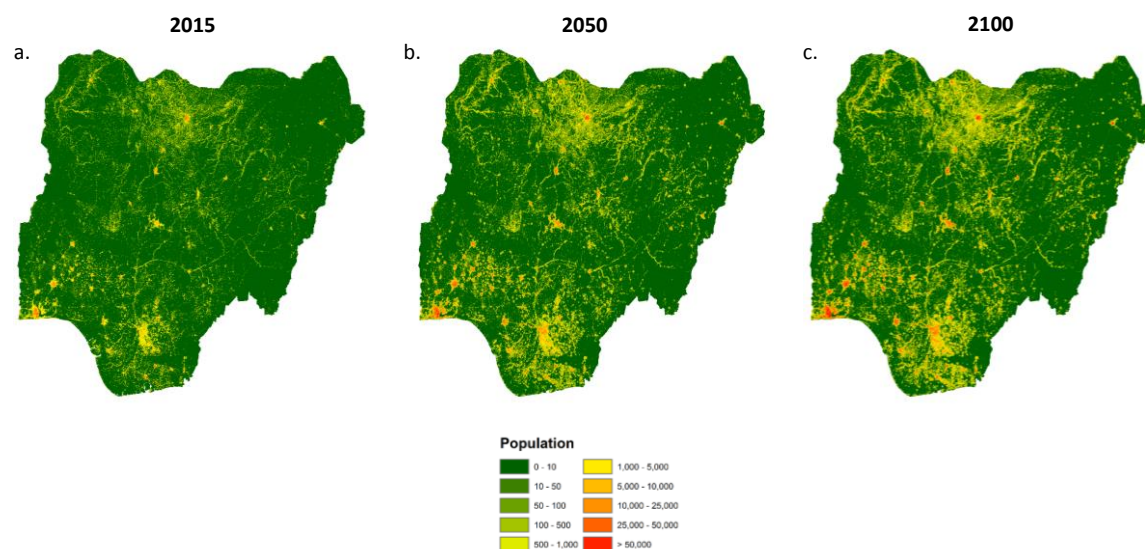


Figure 12. Projected population change, 2050 and 2100: Nigeria SSP2 – Medium Variant

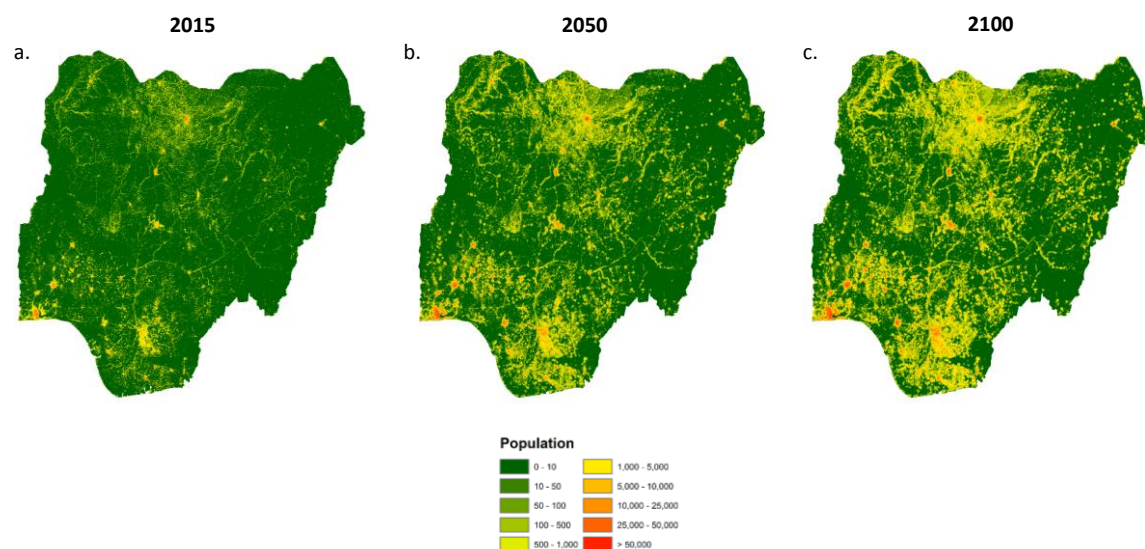


Figure 13. Projected population change, 2050 and 2100: Nigeria SSP2 – Low Variant

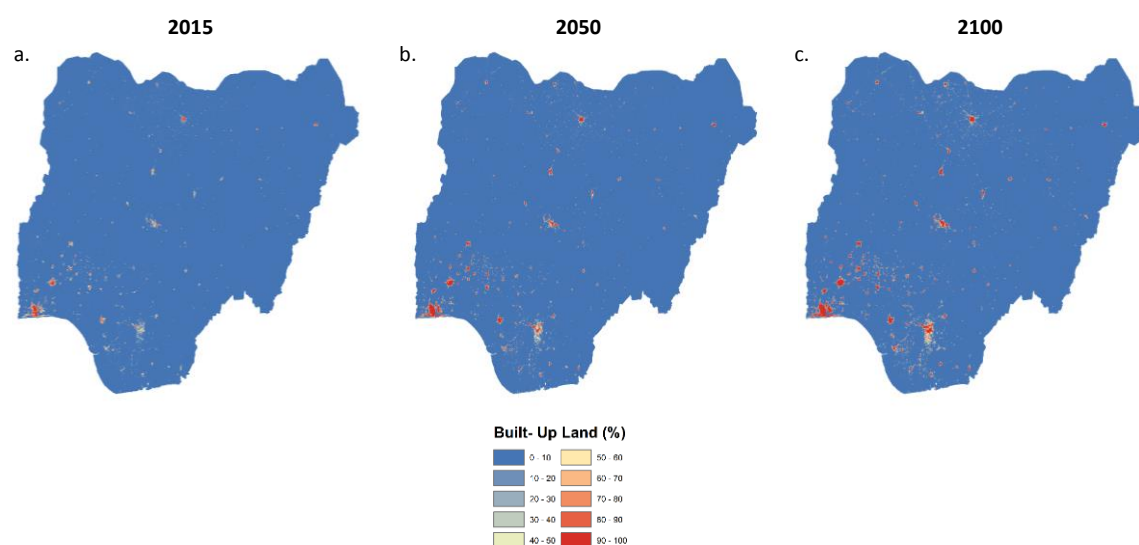


Figure 14. Projected change in built-up land, 2050 and 2100: Nigeria SSP2

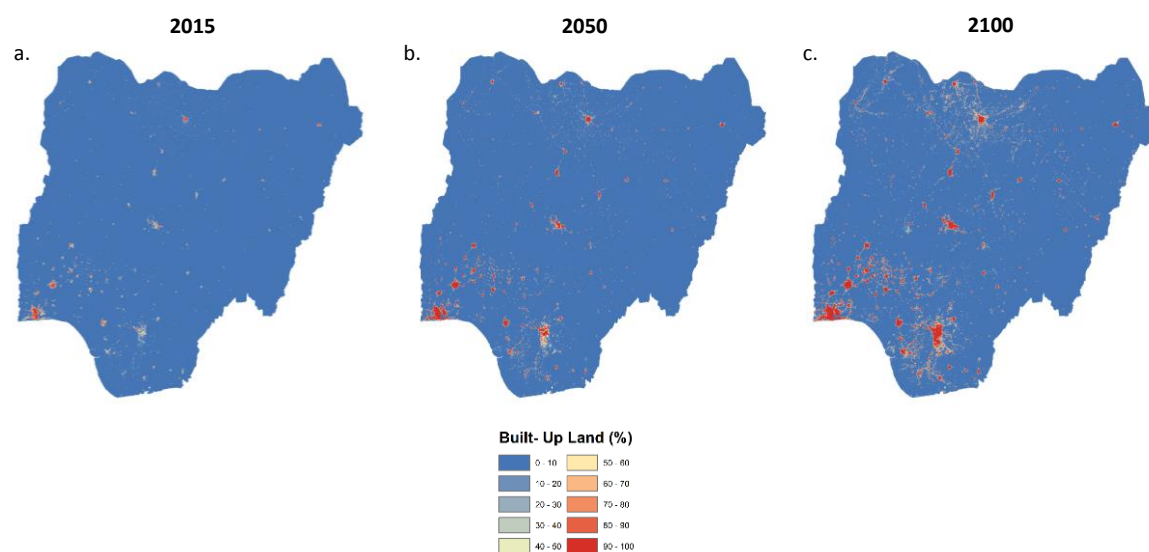


Figure 15. Projected change in built-up land, 2050 and 2100: Nigeria SSP2 – High Variant

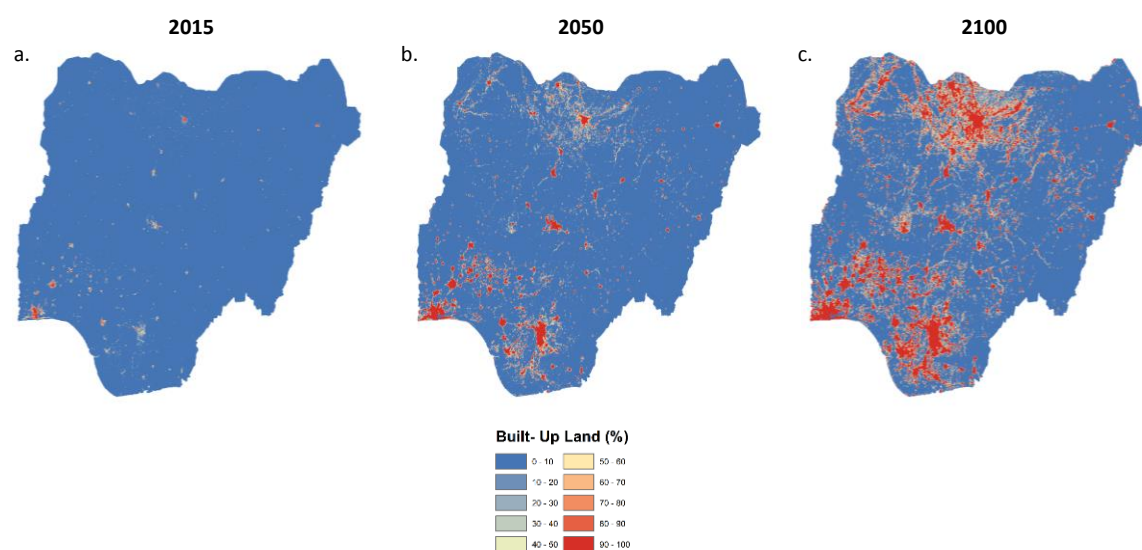


Figure 16. Projected change in built-up land, 2050 and 2100: Nigeria SSP2 – Medium Variant

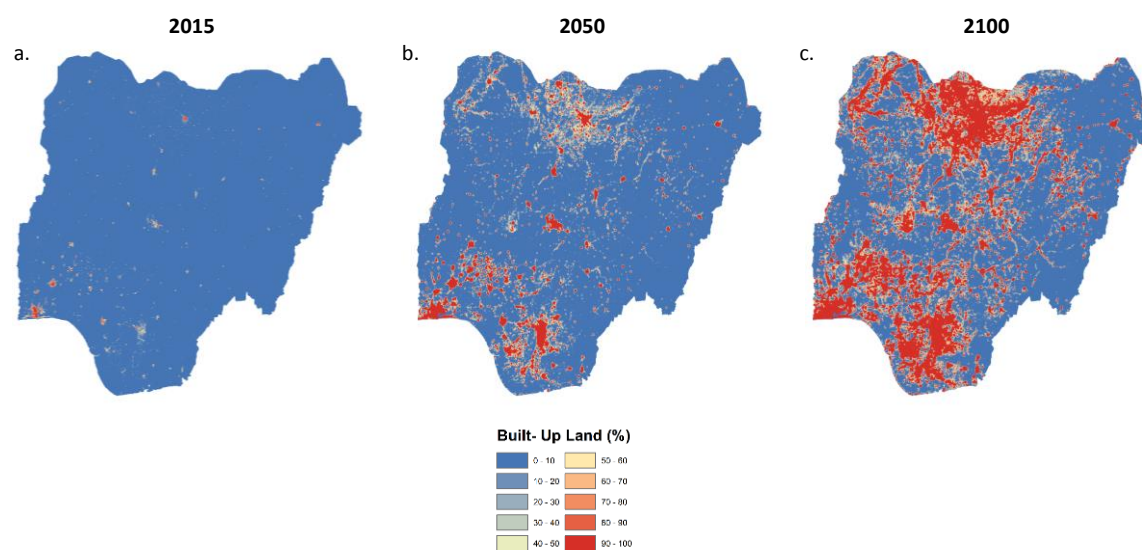


Figure 17. Projected change in built-up land, 2050 and 2100: Nigeria SSP2 – Low Variant

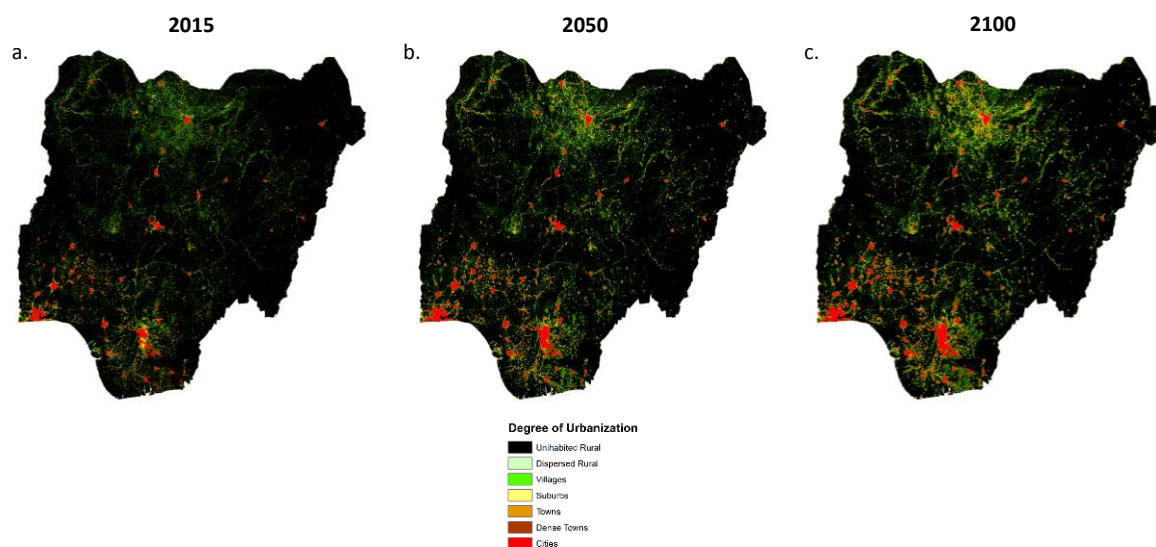


Figure 18. Projected change in degree of urbanization, 2050 and 2100: Nigeria SSP2.

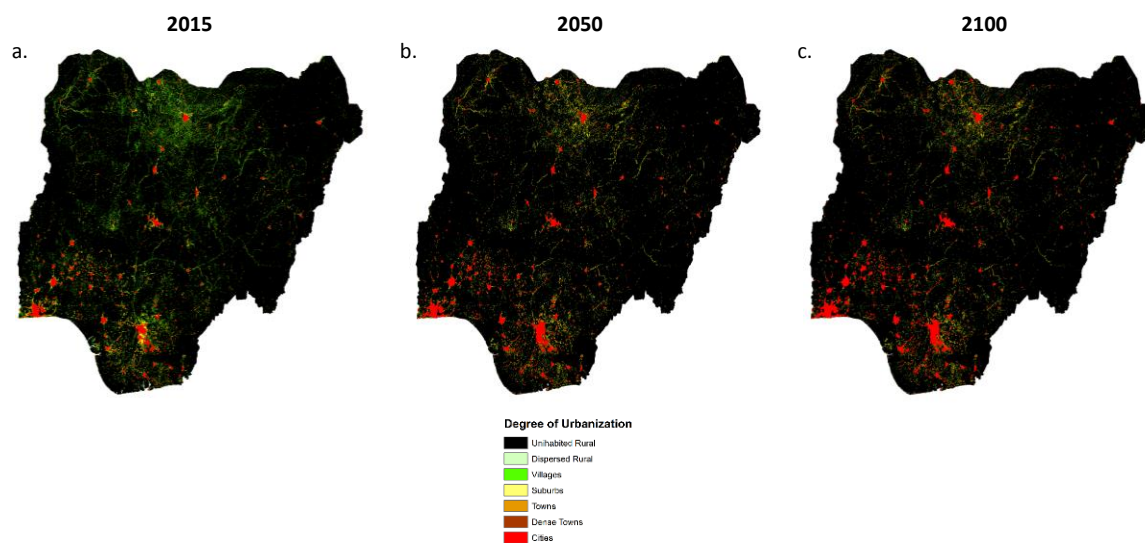


Figure 19. Projected change in degree of urbanization, 2050 and 2100: Nigeria SSP2 – High Variant.

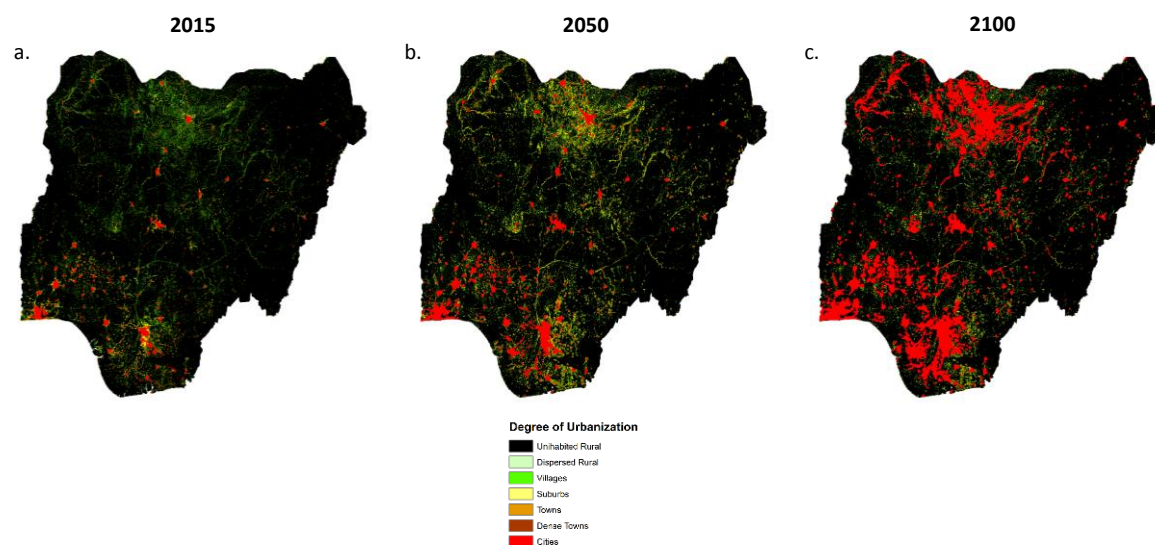


Figure 20. Projected change in degree of urbanization, 2050 and 2100: Nigeria SSP2 – Medium Variant.

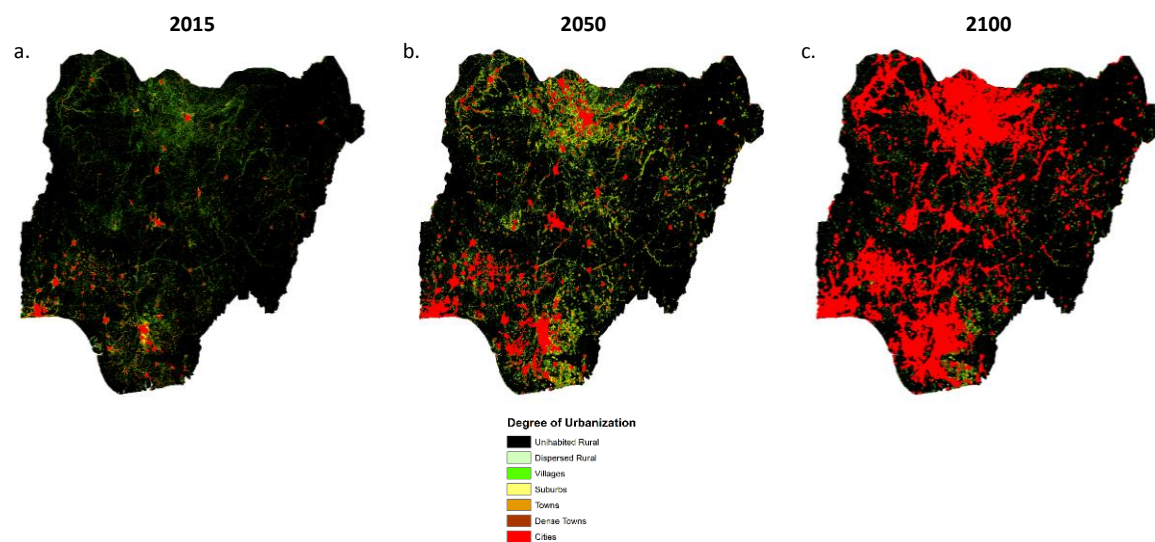


Figure 21. Projected change in degree of urbanization, 2050 and 2100: Nigeria SSP2 – Low Variant.

3.2 Germany

Table 8. Population, land area, and population density by degree of urbanization, SSP2 and variants: Germany 2015 and 2050.

	2015						
	Uninhabited Rural	Dispersed Rural	Villages	Suburbs	Towns	Cities	Total
Area	219,373	86,770	13,310	21,166	10,899	9,056	360,574
Pop	1,735,423	12,376,593	8,231,943	17,320,255	14,718,014	26,367,485	80,749,712
Density	7.91	142.64	618.50	818.29	1350.36	2911.62	223.95

Area	2050						
	Uninhabited Rural	Dispersed Rural	Villages	Suburbs	Towns	Cities	Total
SSP2	232,045	75,143	12,848	20,498	10,499	9,540	360,574
Low	234,479	70,410	12,842	21,455	12,088	9,300	360,574
Medium	240,802	70,822	11,029	17,785	9,621	10,515	360,574
High	316,799	13,489	5,224	5,905	6,711	12,446	360,574

Pop	2050						
	Uninhabited Rural	Dispersed Rural	Villages	Suburbs	Towns	Cities	Total
SSP2	1,254,999	11,036,733	8,067,134	16,791,655	14,429,138	27,352,586	78,932,245
Low	1,292,866	10,220,492	8,988,008	19,835,506	15,105,048	23,490,328	78,932,248
Medium	1,373,506	10,188,729	7,486,564	14,797,607	16,358,459	28,727,381	78,932,246
High	710,958	1,900,618	6,473,742	6,625,903	16,392,607	46,828,416	78,932,244

Density	2050						
	Uninhabited Rural	Dispersed Rural	Villages	Suburbs	Towns	Cities	Total
SSP2	5.41	146.88	627.88	819.19	1374.30	2867.03	218.91
Low	5.51	145.16	699.89	924.52	1249.59	2525.84	218.91
Medium	5.70	143.86	678.81	832.03	1700.29	2732.04	218.91
High	2.24	140.90	1239.23	1122.08	2442.65	3762.53	218.91

Table 9. Population, land area, and population density by degree of urbanization, SSP2 and variants: Germany 2015 and 2100.

	2015						
	Uninhabited Rural	Dispersed Rural	Villages	Suburbs	Towns	Cities	Total
Area	219,373	86,770	13,310	21,166	10,899	9,056	360,574
Pop	1,735,423	12,376,593	8,231,943	17,320,255	14,718,014	26,367,485	80,749,712
Density	7.91	142.64	618.50	818.29	1350.36	2911.62	223.95

Area	2100						
	Uninhabited Rural	Dispersed Rural	Villages	Suburbs	Towns	Cities	Total
SSP2	282,707	33,642	9,827	16,376	8,644	9,379	360,574
Low	234,469	70,386	12,842	21,145	11,985	9,747	360,574
Medium	240,802	70,821	11,029	17,770	9,596	10,556	360,574
High	316,799	13,489	5,224	5,905	6,711	12,446	360,574

Pop	2100						
	Uninhabited Rural	Dispersed Rural	Villages	Suburbs	Towns	Cities	Total
SSP2	328,027	5,581,667	6,774,452	13,938,719	12,944,842	26,959,897	66,527,604
Low	11,176	3,114,624	8,103,133	20,097,772	14,097,269	21,103,627	66,527,602
Medium	9,009	2,931,006	5,726,242	12,931,322	16,717,927	28,212,100	66,527,606
High	185,085	883,305	4,579,530	4,826,061	13,750,703	42,302,924	66,527,608

Density	2100						
	Uninhabited Rural	Dispersed Rural	Villages	Suburbs	Towns	Cities	Total
SSP2	1.16	165.92	689.38	851.16	1497.58	2874.63	184.50
Low	0.05	44.25	630.99	950.47	1176.24	2165.14	184.50
Medium	0.04	41.39	519.20	727.71	1742.18	2672.61	184.50
High	0.58	65.48	876.63	817.28	2048.98	3398.92	184.50

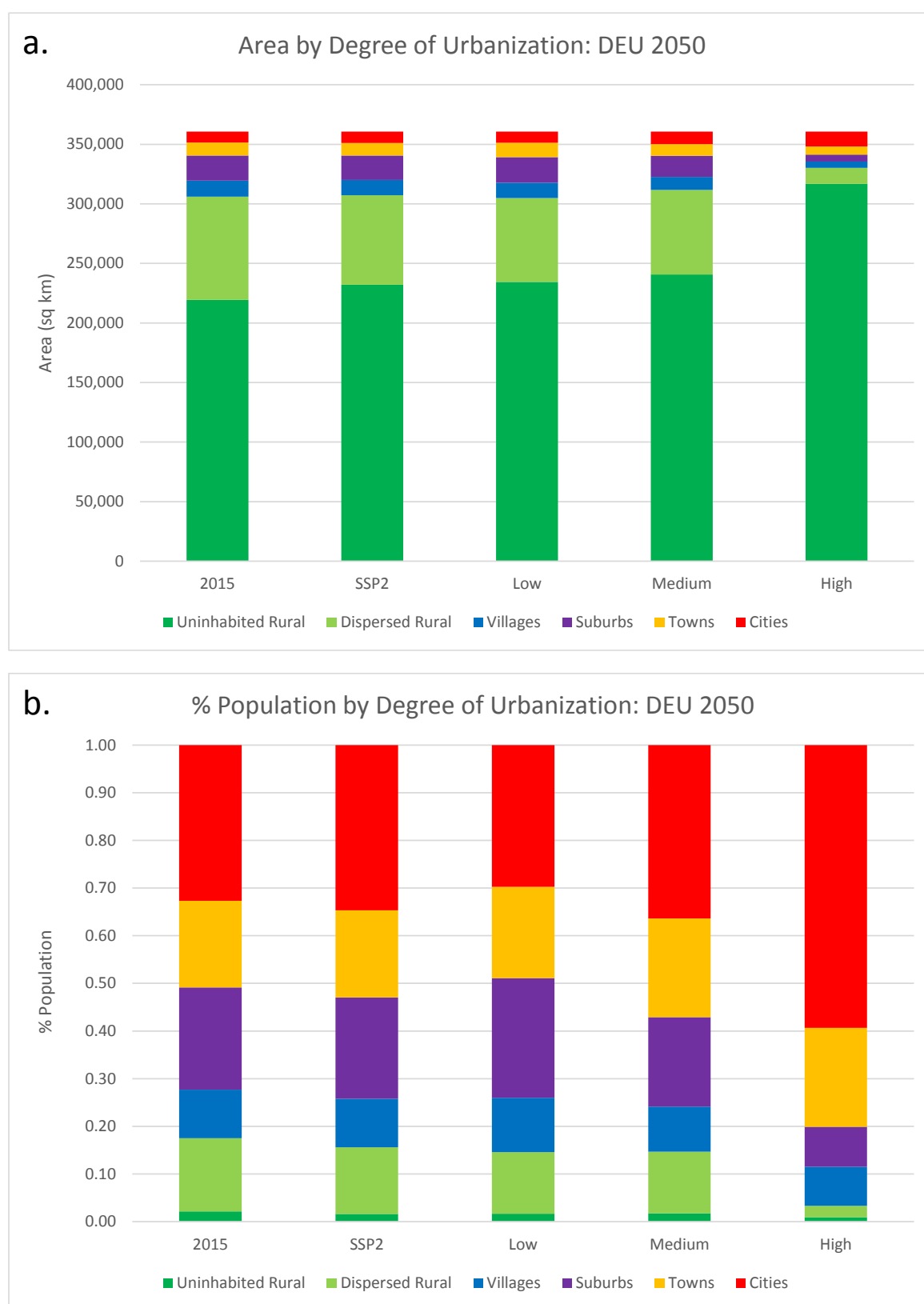


Figure 22. Distribution of (a) land and (b) population by degree of urbanization, SSP2 and variants: Germany 2015 and 2050.

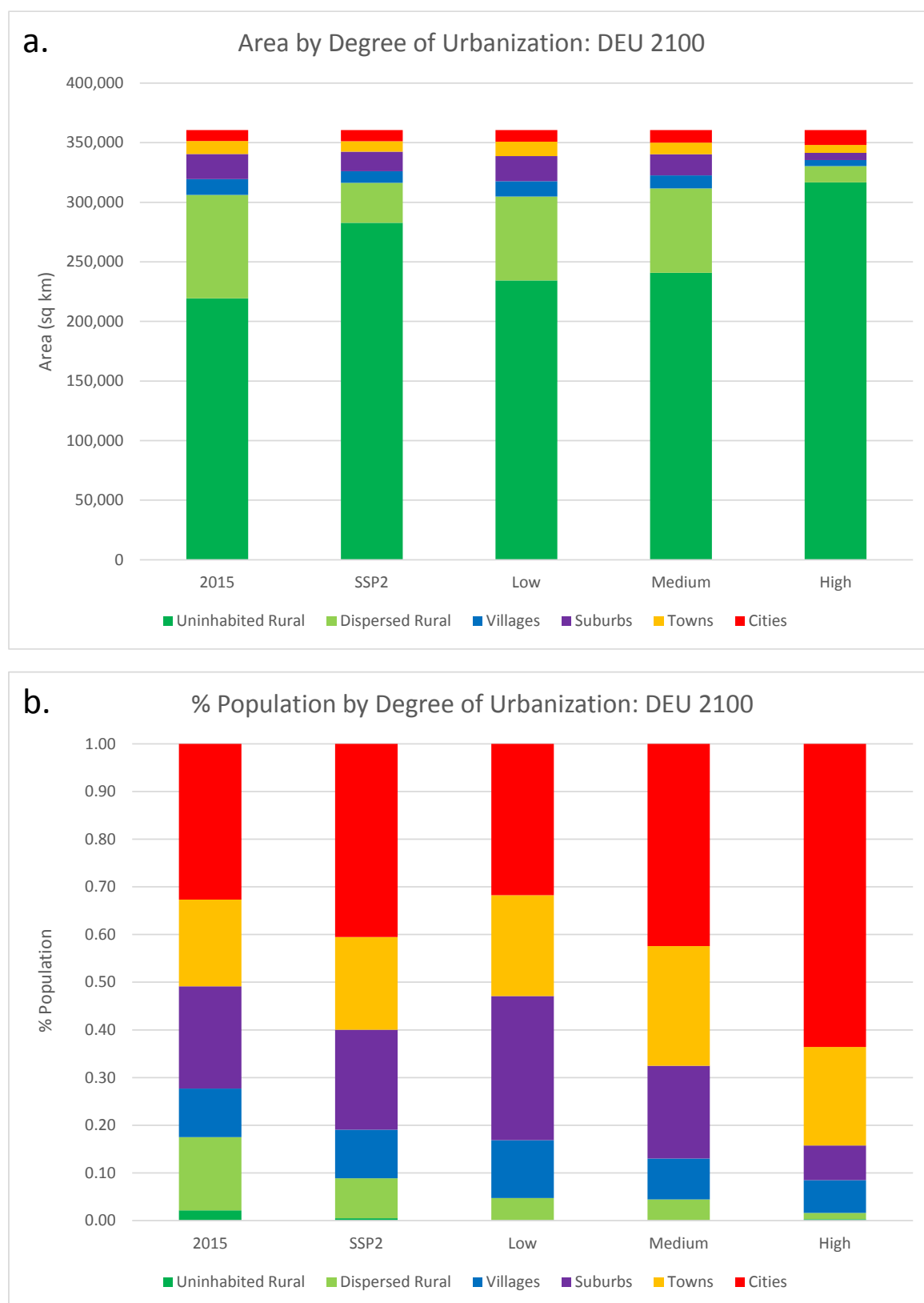


Figure 23. Distribution of (a) land and (b) population by degree of urbanization, SSP2 and variants: Germany 2015 and 2100.

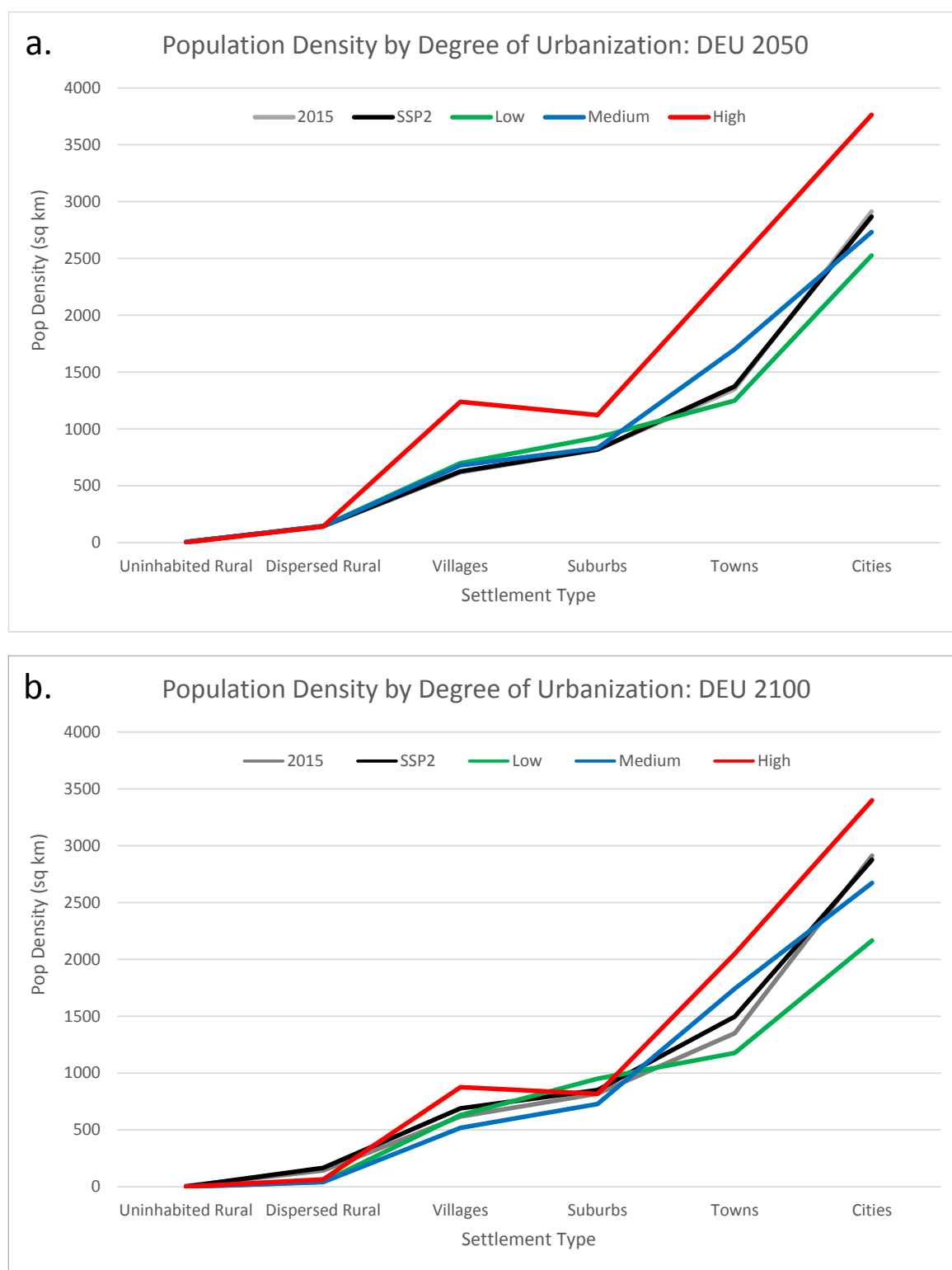


Figure 24. Population density by settlement type for (a) 2015 and 2050 and (b) 2015 and 2100: Germany, SSP2 and variants.

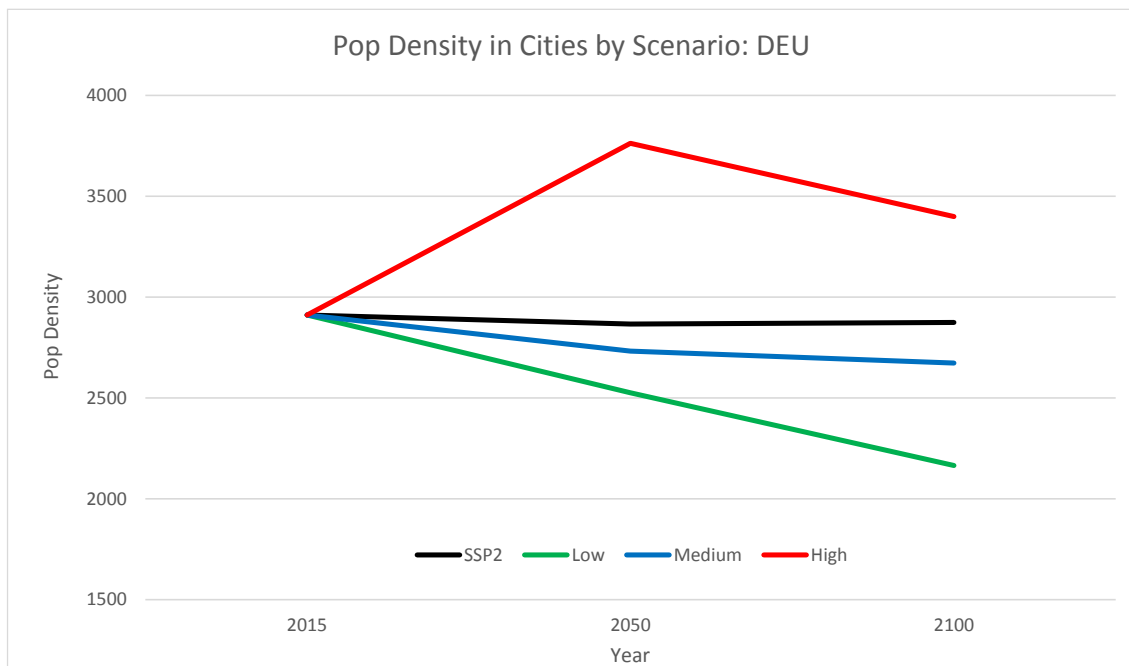


Figure 25. Population density in cities in 2015, 2050, and 2100: Germany, SSP2 and variants.

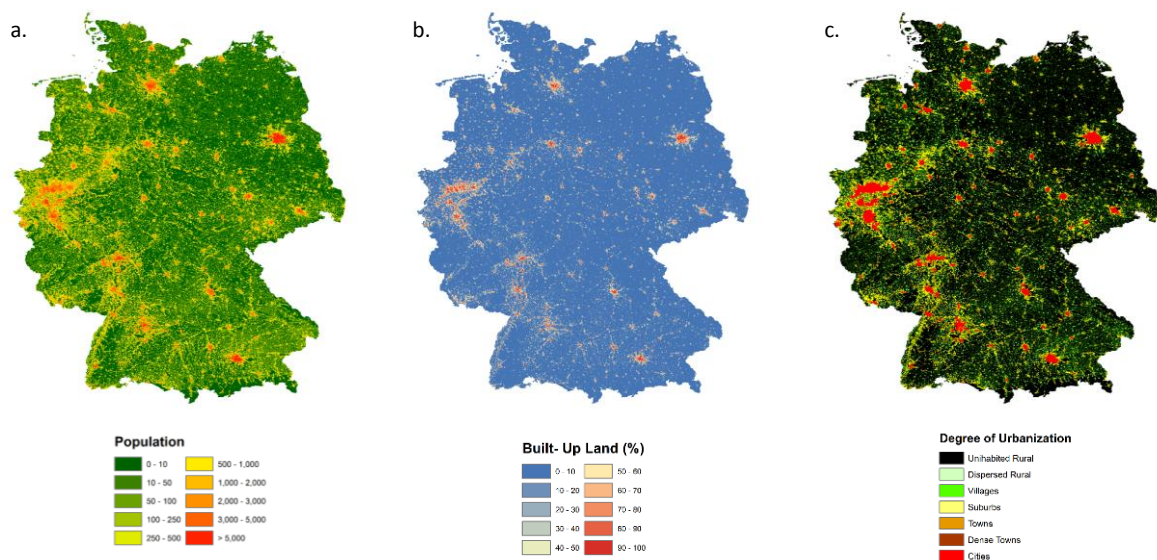


Figure 26. Observed distribution of (a) population, (b) built-up land, and the (c) degree of urbanization; Germany 2015.

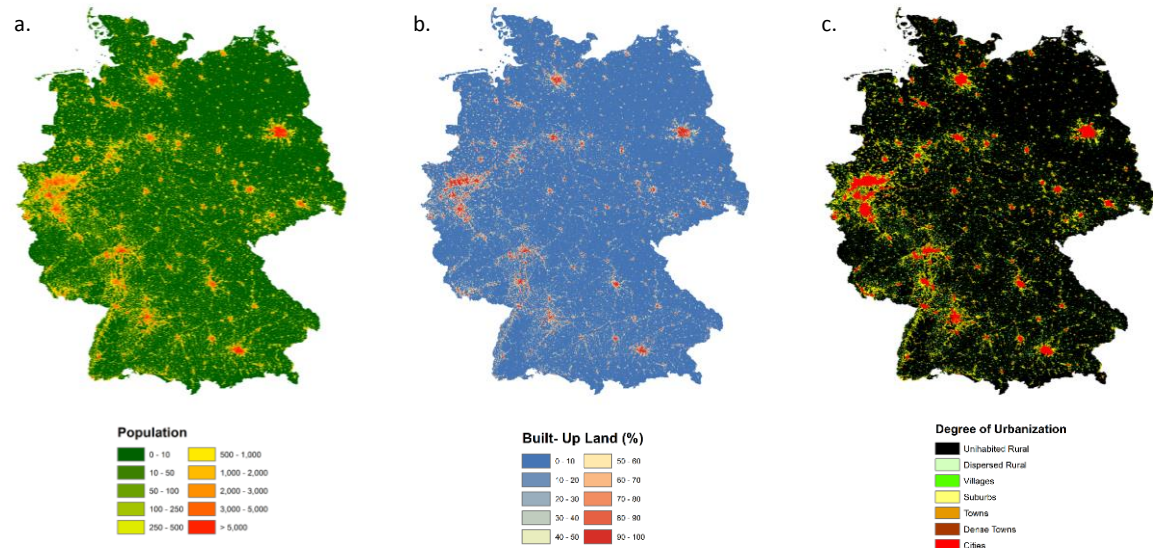


Figure 27. Projected distribution of (a) population, (b) built-up land, and the (c) degree of urbanization; Germany 2100, SSP2.

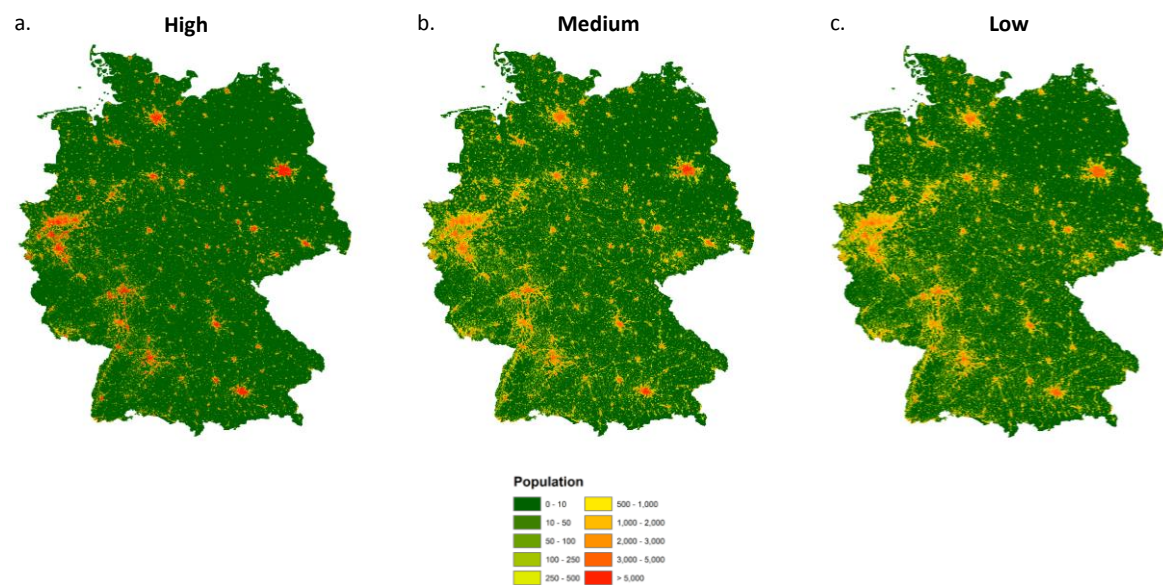


Figure 28. Projected population distribution for the (a) high, (b) medium, and (c) low variants; Germany 2100.

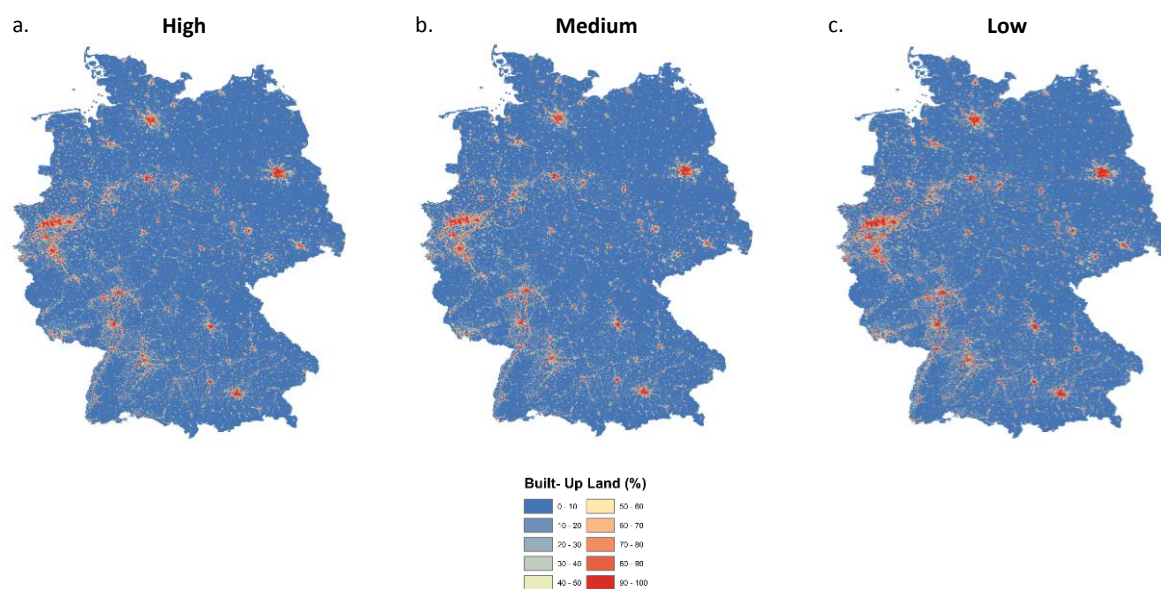


Figure 29. Projected distribution of built-up land for the (a) high, (b) medium, and (c) low variants; Germany 2100.

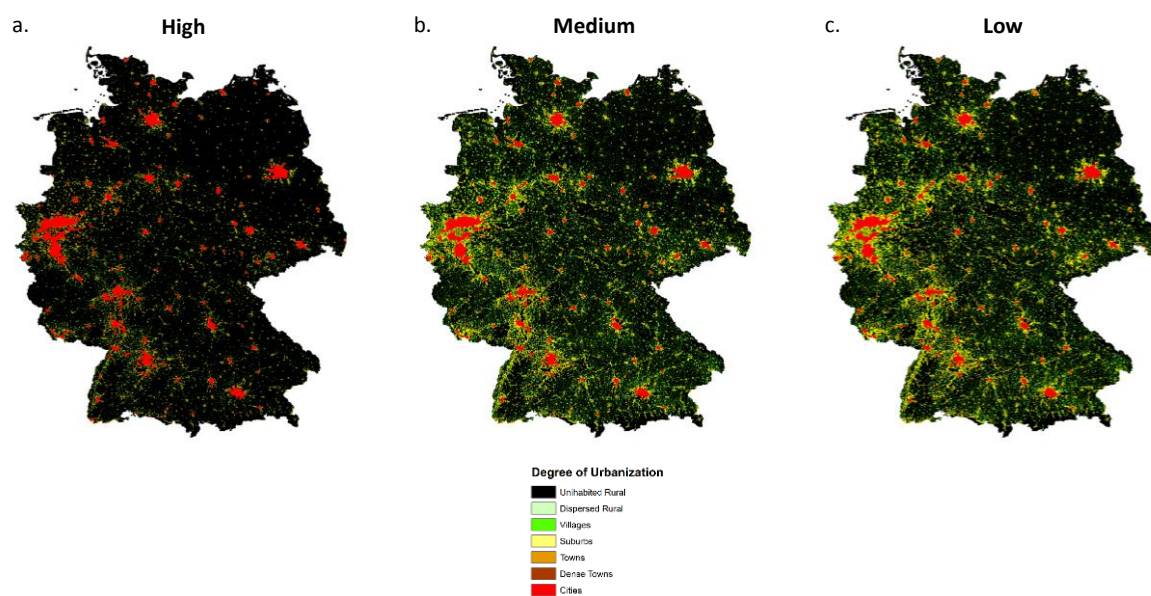


Figure 30. Projected degree of urbanization for the (a) high, (b) medium, and (c) low variants; Germany 2100.

4. Deliverables

The following materials have been delivered to the European Commission:

- 1) Global gridded population projections of SSP2 by country (240 countries and territories) for the period 2020-2100 in 10-year time steps at 1km resolution (GDB format).
- 2) Global gridded population projections of the SSP2 variants by country (240 countries and territories) for 2050 and 2100 at 1km resolution (GDB format).
- 3) Global gridded built-up land projections by country for SSP2 (240 countries and territories) for the period 2020-2100 in 10-year time steps at 1km resolution (GDB format).
- 4) Global gridded built-up land projections by country for the SSP2 variants (240 countries and territories) for 2050 and 2100 at 1km resolution (GDB format).

Additional analysis of model output has led to the sharing of multiple ancillary data products, including:

- Projections of the degree of urbanization
 - Global: 2020-2050
 - Nigeria and Germany: 2020-2100
- Population by degree of urbanization and country: 2020-2050
- Land area by degree of urbanization and country: 2020-2050
- High density clusters, count and total population, by country, 2015-2015

5. References

- [1] Seto, K.C., Guneralp, B. and Hutyrá, L.R. (2012) Global forecasts of urban expansion to 2030 and direct impacts on biodiversity and carbon pools. *Proceedings of the National Academy of Sciences* 109:16083-16088.
- [2] Bierwagen, B.G., Theobald, D.M., Pyke, C.R., Choate, A., Groth, P., Thomas, J.V. and Morefield, P. (2010) National housing and impervious surface scenarios for integrated climate impact assessments. *Proceedings of the National Academy of Sciences*, 107(49):20887-20892.
- [3] Guneralp, B. and Seto, K.C. (2013) Futures of global urban expansion: uncertainties and implications for biodiversity conservation. *Environmental Research Letters*, 8, 014025.
- [4] Ewing R and Rong F (2008) The impact of urban form on US residential energy use. *Housing Policy Debate*, 19(1):1-30.
- [5] Parry, M. L., Rosenzweig, C., Iglesias, A., Livermore, M. and Fischer, G. (2004) Effects of climate change on global food production under SRES emissions and socio-economic scenarios. *Global Environmental Change* 14:53-67.
- [6] McDonald, R.I., Green, P., Balk, D., Fekete, B.M., Revenga, C., Todd, M., Montgomery, M.R. (2011) Urban growth, climate change, and freshwater availability. *Proceedings of the National Academy of Science of the United States of America* 108(15): 6312-6317.
- [7] Arnell, N.W. (2004) Climate change and global water resources: SRES emissions and socio-economic scenarios, *Global Environmental Change*, 14(1):31-52.
- [8] Lamarque, J.F., Bond, T.C., Eyring, V., Heil, A., et al. (2010) Historical (1850-2000) gridded anthropogenic and biomass burning emissions of reactive gases and aerosols: Methodology and application. *Atmospheric Chemistry and Physics*, 10(15):4963-5019.
- [9] Raupach, M.R., Rayner, P.J., Page, M. (2010) Regional variations in spatial structure of nightlights, population density and fossil fuel CO₂ emissions. *Energy Policy*, 38(9):4756-4764.
- [10] Jones, K.E., Patel, N.G., Levy, M.A., Storeygard, A., Balk, D., Gittleman, J.L., Daszak, P. (2008) Global trends in emerging infectious diseases, *Nature* 451 (7181): 990-993.
- [11] Jones, B. and O'Neill, B.C. (2013) Historically grounded spatial population projections for the continental United States. *Environmental Research Letters*, 8(4):044021. doi:10.1088/1748-9326/8/4/044021
- [12] Jones, B. and O'Neill, B.C. (2016) Spatially explicit global population scenarios consistent with the Shared Socioeconomic Pathways. *Environmental Research Letters* 11(8):084003. doi:10.1088/1748-9326/11/8/084003.
- [13] Rigaud, K., de Sherbinin, A., Jones, B., Bergmann, J., Clement, V., Ober, K., Schewe, J., Adamo, S., McCusker, B., Heuser, S., and Midgley, A. (2018) Groundswell: Preparing for Internal Climate Migration. World Bank, Washington, DC.
- [14] O'Neill BC, Kriegler E, Ebi KL et al. (2015) The roads ahead: Narratives for shared socioeconomic pathways describing world futures in the 21st century. *Global Environ Change*. doi:10.1016/j.gloenvcha.2015.01.004
- [15] Schiavina, Marcello; Freire, Sergio; MacManus, Kytt (2019): GHS population grid multitemporal (1975, 1990, 2000, 2015) R2019A. European Commission, Joint Research Centre (JRC) DOI: 10.2905/42E8BE89-54FF-464E-BE7B-BF9E64DA5218 PID: <http://data.europa.eu/89h/0c6b9751-a71f-4062-830b-43c9f432370f>
- [16] Pesaresi, M., Ehrlich, D., Ferri, S., Florczyk, A., Freire, S., Haag, F., Halkia, M., Julea, A.M., Kemper, T., Soille, P., (2015) Global human settlement analysis for disaster risk reduction. *Int. Arch. Photogramm. Remote. Sens. Spat. Inf. Sci.* 40 (7), 837-843.

- [17] Pesaresi, M., Ehrlich, D., Ferri, S., Florczyk, A., Freire, S., Halkia, S., Julea, A., Kemper, T., Soille, P., and Syrris, V. (2016a) Operating procedure for the production of the Global Human Settlement Layer from Landsat data of the epochs 1975, 1990, 2000, and 2014. In: JRC Technical Report EUR 27741 EN, <http://dx.doi.org/10.2788/253582>.
- [18] Pesaresi, M., Syrris, V., and Julea, A. (2016b) A new method for earth observation data analytics based on symbolic machine learning. *Remote Sens.* 8 (5), 399.
- [19] Leyk, S., Uhl, J.H., Balk, D., and Jones, B. (2018) Assessing the Accuracy of Multi-Temporal Built-Up Land Layers across Rural–Urban Trajectories in the United States. *Remote Sensing of the Environment* 204:898-917.
- [20] European Commission, Joint Research Centre (JRC); Columbia University, Center for International Earth Science Information Network - CIESIN (2015): GHS population grid, derived from GPW4, multitemporal (1975, 1990, 2000, 2015). European Commission, Joint Research Centre (JRC) [Dataset] PID: http://data.europa.eu/89h/jrc-ghsl-ghs_pop_gpw4_globe_r2015a.
- [21] DeLorme Publishing Company Inc and ESRI (2013) *World Water Bodies* (Redlands, California: ESRI)
- [22] Danielson J J and Gesch D B (2011) Global multi-resolution terrain elevation data 2010 (GMTED2010): U.S. Geological Survey Open-File Report 2011–1073, 26 p.
- [23] Theilacker J and Anderson K (2010) *Steep Slope Ordinance: A Guide*. Pennsylvania Land Trust Association.
- [24] Houck R (2005) *A Study of Ridgeline and Steep Slope Regulations in Mountain Communities throughout the United States* (Asheville, North Carolina: Land of Sky Regional Council)
- [25] IUCN and UNEP-WCMC (2015) *The World Database on Protected Areas (WDPA) Version 2: March 2015* Cambridge, UK: UNEP-WCMC. Available at: www.protectedplanet.net.
- [26] United Nations Statistical Commission (2020) Report on the fifty-first session. Economic and Social Council. Official Records, 2020, Supplement No. 4.
- [27] European Commission, Degree of Urbanisation overview. Degree of Urbanisation website, <https://ghsl.jrc.ec.europa.eu/degurbaOverview.php>. Accessed on 11/25/2020.
- [28] Rich, D.C. (1978) *Potential Models in Human Geography. Concepts and Techniques in Modern Geography* 26. University of East Anglia, Norwich, England.
- [29] Warntz, W., Wolff, P. (1971) *Breakthroughs in geography*. New York: Plume.
- [30] Center for International Earth Science Information Network - CIESIN - Columbia University. (2017) *Gridded Population of the World, Version 4 (GPWv4): Population Count, Revision 10*. Palisades, NY: NASA Socioeconomic Data and Applications Center (SEDAC). <https://doi.org/10.7927/H4PG1PPM>.
- [31] Balk, D., Leyk, S., Jones, B., Montgomery, M.R. and Clark, A. (2018) Understanding urbanization: A study of census and satellite-derived urban classes in the United States, 1990-2010. *PloS one* 13(12), p.e0208487.
- [32] Clark, C. (1951). Urban Population Densities. *Journal of the Royal Statistical Society. Series A (General)* 114:490-496.
- [33] Bertaud, A., Malpezzi, S. (2003) *The Spatial Distribution of Population in 48 World Cities: Implications for Economies in Transition*. The Center for Urban Land Economics Research, University of Wisconsin. Available

ANNEX A: Countries and territories

Appendix A includes the list of countries and territories independently modelled in this work, by region, the source of the national-level population projection for each country/territory, and the built-up land scenarios modelled for each country/territory.

Region	ISO Code	Country/Territory	Population Projection Source	Built-up Land Scenarios
Australia/New Zealand				
	AUS	Australia	SSP2 - IIASA/WIC	SSP2 and Variants
	CCK	Cocos Islands	Constant*	None
	CXR	Christmas Island	Constant*	None
	NFK	Norfolk Island	Constant*	Constant
	NZL	New Zealand	SSP2 - IIASA/WIC	SSP2 and Variants
Caribbean				
	ABW	Aruba	SSP2 - IIASA/WIC	SSP2 and Variants
	AIA	Anguilla	UN	SSP2 and Variants
	ATG	Antigua and Barbuda	UN	SSP2 and Variants
	BES	Bonaire Saint Eustatius and Saba	UN	SSP2 and Variants
	BHS	Bahamas	SSP2 - IIASA/WIC	SSP2 and Variants
	BLM	Saint-Barthelemy	UN	SSP2 and Variants
	BRB	Barbados	SSP2 - IIASA/WIC	SSP2 and Variants
	CUB	Cuba	SSP2 - IIASA/WIC	SSP2 and Variants
	CUW	Curacao	UN	SSP2 and Variants
	CYM	Cayman Islands	UN	SSP2 and Variants
	DMA	Dominica	UN	SSP2 and Variants
	DOM	Dominican Republic	SSP2 - IIASA/WIC	SSP2 and Variants
	GLP	Guadeloupe	SSP2 - IIASA/WIC	SSP2 and Variants
	GRD	Grenada	SSP2 - IIASA/WIC	SSP2 and Variants
	HTI	Haiti	SSP2 - IIASA/WIC	SSP2 and Variants
	JAM	Jamaica	SSP2 - IIASA/WIC	SSP2 and Variants
	KNA	Saint Kitts and Nevis	UN	SSP2 and Variants
	LCA	Saint Lucia	SSP2 - IIASA/WIC	SSP2 and Variants
	MAF	Saint-Martin (French part)	UN	SSP2 and Variants
	MSR	Montserrat	UN	SSP2 and Variants
	MTQ	Martinique	SSP2 - IIASA/WIC	SSP2 and Variants
	PRI	Puerto Rico	SSP2 - IIASA/WIC	SSP2 and Variants
	SXM	Sint Maarten (Dutch part)	UN	SSP2 and Variants
	TCA	Turks and Caicos Islands	UN	SSP2 and Variants
	TTO	Trinidad and Tobago	SSP2 - IIASA/WIC	SSP2 and Variants
	VCT	Saint Vincent and the Grenadines	SSP2 - IIASA/WIC	SSP2 and Variants
	VGB	British Virgin Islands	UN	SSP2 and Variants
	VIR	United States Virgin Islands	SSP2 - IIASA/WIC	SSP2 and Variants

Central Africa			
AGO	Angola	SSP2 - IIASA/WIC	SSP2 and Variants
CAF	Central African Republic	SSP2 - IIASA/WIC	SSP2 and Variants
CMR	Cameroon	SSP2 - IIASA/WIC	SSP2 and Variants
COD	Democratic Republic of the Congo	SSP2 - IIASA/WIC	SSP2 and Variants
COG	Congo	SSP2 - IIASA/WIC	SSP2 and Variants
GAB	Gabon	SSP2 - IIASA/WIC	SSP2 and Variants
GNQ	Equatorial Guinea	SSP2 - IIASA/WIC	SSP2 and Variants
STP	Sao Tome and Principe	SSP2 - IIASA/WIC	SSP2 and Variants
TCD	Chad	SSP2 - IIASA/WIC	SSP2 and Variants
Central America			
BLZ	Belize	SSP2 - IIASA/WIC	SSP2 and Variants
CRI	Costa Rica	SSP2 - IIASA/WIC	SSP2 and Variants
GTM	Guatemala	SSP2 - IIASA/WIC	SSP2 and Variants
HND	Honduras	SSP2 - IIASA/WIC	SSP2 and Variants
MEX	Mexico	SSP2 - IIASA/WIC	SSP2 and Variants
NIC	Nicaragua	SSP2 - IIASA/WIC	SSP2 and Variants
PAN	Panama	SSP2 - IIASA/WIC	SSP2 and Variants
SLV	El Salvador	SSP2 - IIASA/WIC	SSP2 and Variants
Central Asia			
KAZ	Kazakhstan	SSP2 - IIASA/WIC	SSP2 and Variants
KGZ	Kyrgyzstan	SSP2 - IIASA/WIC	SSP2 and Variants
TJK	Tajikistan	SSP2 - IIASA/WIC	SSP2 and Variants
TKM	Turkmenistan	SSP2 - IIASA/WIC	SSP2 and Variants
UZB	Uzbekistan	SSP2 - IIASA/WIC	SSP2 and Variants
East Africa			
BDI	Burundi	SSP2 - IIASA/WIC	SSP2 and Variants
COM	Comoros	SSP2 - IIASA/WIC	SSP2 and Variants
DJI	Djibouti	SSP2 - IIASA/WIC	SSP2 and Variants
ERI	Eritrea	SSP2 - IIASA/WIC	SSP2 and Variants
ETH	Ethiopia	SSP2 - IIASA/WIC	SSP2 and Variants
KEN	Kenya	SSP2 - IIASA/WIC	SSP2 and Variants
MDG	Madagascar	SSP2 - IIASA/WIC	SSP2 and Variants
MOZ	Mozambique	SSP2 - IIASA/WIC	SSP2 and Variants
MUS	Mauritius	SSP2 - IIASA/WIC	SSP2 and Variants
MWI	Malawi	SSP2 - IIASA/WIC	SSP2 and Variants
MYT	Mayotte	SSP2 - IIASA/WIC	SSP2 and Variants
REU	Reunion	SSP2 - IIASA/WIC	SSP2 and Variants
RWA	Rwanda	SSP2 - IIASA/WIC	SSP2 and Variants
SOM	Somalia	SSP2 - IIASA/WIC	SSP2 and Variants
SYC	Seychelles	UN	SSP2 and Variants
TZA	United Republic of Tanzania	SSP2 - IIASA/WIC	SSP2 and Variants
UGA	Uganda	SSP2 - IIASA/WIC	SSP2 and Variants
ZMB	Zambia	SSP2 - IIASA/WIC	SSP2 and Variants
ZWE	Zimbabwe	SSP2 - IIASA/WIC	SSP2 and Variants

East Asia			
CHN	China	SSP2 - IIASA/WIC	SSP2 and Variants
HKG	Hong Kong	SSP2 - IIASA/WIC	SSP2 and Variants
JPN	Japan	SSP2 - IIASA/WIC	SSP2 and Variants
KOR	Republic of Korea	SSP2 - IIASA/WIC	SSP2 and Variants
MAC	Macao	SSP2 - IIASA/WIC	SSP2 and Variants
MNG	Mongolia	SSP2 - IIASA/WIC	SSP2 and Variants
PIS	Paracel Islands	Constant*	None
PRK	Democratic People's Republic of Korea	SSP2 - IIASA/WIC	SSP2 and Variants
TWN	Taiwan	SSP2 - IIASA/WIC	SSP2 and Variants
Eastern Europe			
BGR	Bulgaria	SSP2 - IIASA/WIC	SSP2 and Variants
BLR	Belarus	SSP2 - IIASA/WIC	SSP2 and Variants
CZE	Czech Republic	SSP2 - IIASA/WIC	SSP2 and Variants
HUN	Hungary	SSP2 - IIASA/WIC	SSP2 and Variants
MDA	Republic of Moldova	SSP2 - IIASA/WIC	SSP2 and Variants
POL	Poland	SSP2 - IIASA/WIC	SSP2 and Variants
ROU	Romania	SSP2 - IIASA/WIC	SSP2 and Variants
RUS	Russian Federation	SSP2 - IIASA/WIC	SSP2 and Variants
SVK	Slovakia	SSP2 - IIASA/WIC	SSP2 and Variants
UKR	Ukraine	SSP2 - IIASA/WIC	SSP2 and Variants
North Africa			
DZA	Algeria	SSP2 - IIASA/WIC	SSP2 and Variants
EGY	Egypt	SSP2 - IIASA/WIC	SSP2 and Variants
ESH	Western Sahara	SSP2 - IIASA/WIC	SSP2 and Variants
LBY	Libya	SSP2 - IIASA/WIC	SSP2 and Variants
MAR	Morocco	SSP2 - IIASA/WIC	SSP2 and Variants
SDN	Sudan**	SSP2 - IIASA/WIC	SSP2 and Variants
TUN	Tunisia	SSP2 - IIASA/WIC	SSP2 and Variants
North America			
BMU	Bermuda	UN	SSP2 and Variants
CAN	Canada	SSP2 - IIASA/WIC	SSP2 and Variants
GRL	Greenland	UN	SSP2 and Variants
SPM	Saint Pierre and Miquelon	UN	SSP2 and Variants
USA	USA	SSP2 - IIASA/WIC	SSP2 and Variants
Northern Europe			
DNK	Denmark	SSP2 - IIASA/WIC	SSP2 and Variants
EST	Estonia	SSP2 - IIASA/WIC	SSP2 and Variants
FIN	Finland	SSP2 - IIASA/WIC	SSP2 and Variants
FRO	Faeroe Islands	UN	None
ISL	Iceland	SSP2 - IIASA/WIC	SSP2 and Variants
LTU	Lithuania	SSP2 - IIASA/WIC	SSP2 and Variants
LVA	Latvia	SSP2 - IIASA/WIC	SSP2 and Variants
NOR	Norway	SSP2 - IIASA/WIC	SSP2 and Variants
SJM	Svalbard and Jan Mayen	Constant*	
SWE	Sweden	SSP2 - IIASA/WIC	SSP2 and Variants

Pacific Islands			
ASM	American Samoa	UN	SSP2 and Variants
COK	Cook Islands	UN	SSP2 and Variants
FJI	Fiji	SSP2 - IIASA/WIC	SSP2 and Variants
FSM	Micronesia (Federated States of)	SSP2 - IIASA/WIC	SSP2 and Variants
GUM	Guam	SSP2 - IIASA/WIC	SSP2 and Variants
KIR	Kiribati	UN	SSP2 and Variants
MHL	Marshall Islands	UN	SSP2 and Variants
MNP	Northern Mariana Islands	UN	SSP2 and Variants
NCL	New Caledonia	SSP2 - IIASA/WIC	SSP2 and Variants
NIU	Niue	UN	None
NRU	Nauru	UN	SSP2 and Variants
PCN	Pitcairn Island	Constant*	SSP2 and Variants
PLW	Palau	UN	SSP2 and Variants
PYF	French Polynesia	UN	SSP2 and Variants
SLB	Solomon Islands	SSP2 - IIASA/WIC	SSP2 and Variants
TKL	Tokelau	UN	None
TON	Tonga	SSP2 - IIASA/WIC	SSP2 and Variants
TUV	Tuvalu	UN	SSP2 and Variants
VUT	Vanuatu	SSP2 - IIASA/WIC	SSP2 and Variants
WLF	Wallis and Futuna Islands	UN	SSP2 and Variants
WSM	Western Samoa	SSP2 - IIASA/WIC	SSP2 and Variants
South Africa			
BWA	Botswana	SSP2 - IIASA/WIC	SSP2 and Variants
LSO	Lesotho	SSP2 - IIASA/WIC	SSP2 and Variants
NAM	Namibia	SSP2 - IIASA/WIC	SSP2 and Variants
SWZ	Swaziland	SSP2 - IIASA/WIC	SSP2 and Variants
ZAF	South_Africa	SSP2 - IIASA/WIC	SSP2 and Variants
South America			
ARG	Argentina	SSP2 - IIASA/WIC	SSP2 and Variants
BOL	Bolivia	SSP2 - IIASA/WIC	SSP2 and Variants
BRA	Brazil	SSP2 - IIASA/WIC	SSP2 and Variants
CHL	Chile	SSP2 - IIASA/WIC	SSP2 and Variants
COL	Colombia	SSP2 - IIASA/WIC	SSP2 and Variants
ECU	Ecuador	SSP2 - IIASA/WIC	SSP2 and Variants
FLK	Falkland Islands (Malvinas)	UN	SSP2 and Variants
GUF	French Guiana	SSP2 - IIASA/WIC	SSP2 and Variants
GUY	Guyana	SSP2 - IIASA/WIC	SSP2 and Variants
PER	Peru	SSP2 - IIASA/WIC	SSP2 and Variants
PRY	Paraguay	SSP2 - IIASA/WIC	SSP2 and Variants
SUR	Suriname	SSP2 - IIASA/WIC	SSP2 and Variants
URY	Uruguay	SSP2 - IIASA/WIC	SSP2 and Variants
VEN	Venezuela (Bolivarian Republic of)	SSP2 - IIASA/WIC	SSP2 and Variants

South Asia			
AFG	Afghanistan	SSP2 - IIASA/WIC	SSP2 and Variants
BGD	Bangladesh	SSP2 - IIASA/WIC	SSP2 and Variants
BTN	Bhutan	SSP2 - IIASA/WIC	SSP2 and Variants
IND	India	SSP2 - IIASA/WIC	SSP2 and Variants
IRN	Iran	SSP2 - IIASA/WIC	SSP2 and Variants
LKA	Sri Lanka	SSP2 - IIASA/WIC	SSP2 and Variants
MDV	Maldives	SSP2 - IIASA/WIC	SSP2 and Variants
NPL	Nepal	SSP2 - IIASA/WIC	SSP2 and Variants
PAK	Pakistan	SSP2 - IIASA/WIC	SSP2 and Variants
Southeast Asia			
BRN	Brunei Darussalam	SSP2 - IIASA/WIC	SSP2 and Variants
IDN	Indonesia	SSP2 - IIASA/WIC	SSP2 and Variants
KHM	Cambodia	SSP2 - IIASA/WIC	SSP2 and Variants
LAO	Laos	SSP2 - IIASA/WIC	SSP2 and Variants
MMR	Myanmar	SSP2 - IIASA/WIC	SSP2 and Variants
MYS	Malaysia	SSP2 - IIASA/WIC	SSP2 and Variants
PHL	Philippines	SSP2 - IIASA/WIC	SSP2 and Variants
PNG	Papua New Guinea	SSP2 - IIASA/WIC	SSP2 and Variants
SGP	Singapore	SSP2 - IIASA/WIC	SSP2 and Variants
THA	Thailand	SSP2 - IIASA/WIC	SSP2 and Variants
TLS	Timor-Leste	SSP2 - IIASA/WIC	SSP2 and Variants
VNM	Vietnam	SSP2 - IIASA/WIC	SSP2 and Variants
Southern Europe			
ALB	Albania	SSP2 - IIASA/WIC	SSP2 and Variants
AND	Andorra	UN	SSP2 and Variants
BIH	Bosnia and Herzegovina	SSP2 - IIASA/WIC	SSP2 and Variants
ESP	Spain	SSP2 - IIASA/WIC	SSP2 and Variants
GIB	Gibraltar	UN	SSP2 and Variants
GRC	Greece	SSP2 - IIASA/WIC	SSP2 and Variants
HRV	Croatia	SSP2 - IIASA/WIC	SSP2 and Variants
ITA	Italy	SSP2 - IIASA/WIC	SSP2 and Variants
MKD	Macedonia	SSP2 - IIASA/WIC	SSP2 and Variants
MLT	Malta	SSP2 - IIASA/WIC	SSP2 and Variants
MNE	Montenegro	SSP2 - IIASA/WIC	SSP2 and Variants
PRT	Portugal	SSP2 - IIASA/WIC	SSP2 and Variants
SMR	San Marino	UN	SSP2 and Variants
SRB	Serbia	SSP2 - IIASA/WIC	SSP2 and Variants
SVN	Slovenia	SSP2 - IIASA/WIC	SSP2 and Variants

West Africa			
BEN	Benin	SSP2 - IIASA/WIC	SSP2 and Variants
BFA	Burkina Faso	SSP2 - IIASA/WIC	SSP2 and Variants
CIV	Cote d'Ivoire	SSP2 - IIASA/WIC	SSP2 and Variants
CPV	Cape Verde	SSP2 - IIASA/WIC	SSP2 and Variants
GHA	Ghana	SSP2 - IIASA/WIC	SSP2 and Variants
GIN	Guinea	SSP2 - IIASA/WIC	SSP2 and Variants
GMB	Gambia	SSP2 - IIASA/WIC	SSP2 and Variants
GNB	Guinea-Bissau	SSP2 - IIASA/WIC	SSP2 and Variants
LBR	Liberia	SSP2 - IIASA/WIC	SSP2 and Variants
MLI	Mali	SSP2 - IIASA/WIC	SSP2 and Variants
MRT	Mauritania	SSP2 - IIASA/WIC	SSP2 and Variants
NER	Niger	SSP2 - IIASA/WIC	SSP2 and Variants
NGA	Nigeria	SSP2 - IIASA/WIC	SSP2 and Variants
SEN	Senegal	SSP2 - IIASA/WIC	SSP2 and Variants
SHN	Saint Helena	UN	SSP2 and Variants
SLE	Sierra Leone	SSP2 - IIASA/WIC	SSP2 and Variants
TGO	Togo	SSP2 - IIASA/WIC	SSP2 and Variants
West Asia			
ARE	United Arab Emirates	SSP2 - IIASA/WIC	SSP2 and Variants
ARM	Armenia	SSP2 - IIASA/WIC	SSP2 and Variants
AZE	Azerbaijan	SSP2 - IIASA/WIC	SSP2 and Variants
BHR	Bahrain	SSP2 - IIASA/WIC	SSP2 and Variants
CYP	Cyprus***	SSP2 - IIASA/WIC	SSP2 and Variants
GEO	Georgia	SSP2 - IIASA/WIC	SSP2 and Variants
IRQ	Iraq	SSP2 - IIASA/WIC	SSP2 and Variants
ISR	Israel	SSP2 - IIASA/WIC	SSP2 and Variants
JOR	Jordan	SSP2 - IIASA/WIC	SSP2 and Variants
KWT	Kuwait	SSP2 - IIASA/WIC	SSP2 and Variants
LBN	Lebanon	SSP2 - IIASA/WIC	SSP2 and Variants
OMN	Oman	SSP2 - IIASA/WIC	SSP2 and Variants
PSE	Palestine	SSP2 - IIASA/WIC	SSP2 and Variants
QAT	Qatar	SSP2 - IIASA/WIC	SSP2 and Variants
SAU	Saudi Arabia	SSP2 - IIASA/WIC	SSP2 and Variants
SYR	Syria	SSP2 - IIASA/WIC	SSP2 and Variants
TUR	Turkey	SSP2 - IIASA/WIC	SSP2 and Variants
YEM	Yemen	SSP2 - IIASA/WIC	SSP2 and Variants

Western Europe			
AUT	Austria	SSP2 - IIASA/WIC	SSP2 and Variants
BEL	Belgium	SSP2 - IIASA/WIC	SSP2 and Variants
CHE	Switzerland	SSP2 - IIASA/WIC	SSP2 and Variants
DEU	Germany	SSP2 - IIASA/WIC	SSP2 and Variants
FRA	France	SSP2 - IIASA/WIC	SSP2 and Variants
GBR	United Kingdom	SSP2 - IIASA/WIC	SSP2 and Variants
GGY	Guernsey****	UN	SSP2 and Variants
IMN	Isle of Man	UN	SSP2 and Variants
IRL	Ireland	SSP2 - IIASA/WIC	SSP2 and Variants
JEY	Jersey****	UN	SSP2 and Variants
LIE	Liechtenstein	UN	SSP2 and Variants
LUX	Luxembourg	SSP2 - IIASA/WIC	SSP2 and Variants
MCO	Monaco	UN	SSP2 and Variants
NLD	Netherlands	SSP2 - IIASA/WIC	SSP2 and Variants
<p>* Population is held constant at the observed level from GHS-Pop 2015</p> <p>** Sudan includes South Sudan, as the SSPs do not include independent projections</p> <p>*** Cyprus includes North Cyprus, as the SSPs do not include independent projections</p> <p>**** The UN projects the Channel Islands together, we separate Jersey and Guernsey according to the proportion in each territory in the base year (2015)</p>			

ANNEX B: Data descriptions

Population Projections

Description: The population projection dataset includes population counts by 1km grid-cell. The primary SSP2 dataset includes projections for each 10-year interval over the period 2020-2100. The three variants of SSP2 include projections for 2050 and 2100 only. For reference, the base-year (2015 observed GHS-POP) is included. The data are organized by country/region (regions are delineated in Annex A). Population totals are consistent at the national-level with the SSP2 projection from the SSP database: (<https://tntcat.iiasa.ac.at/SspDb/dsd?Action=htmlpage&page=10>).

Source Files:

SSP2: Pop_builtup_projections_SSP2_2015_2100
Variants: Pop_Builtup_Variants_2050_2100

File names:

SSP2: XXX_POPProject_2015_2100.gdb\PopYEAR

XXX: Three character ISO code

YEAR: Four-digit year

Variants: XXX_POPProject_V_2050_2100.gdb\XXX_PopYEAR

XXX: Three character ISO code

V: Variant - will be one of three letters (H: High, M: Medium, L: Low)

YEAR: Four-digit year

File type: File Geodatabase Raster Dataset

Coordinate System: World Mollweide (EPSG:54009)

Spatial Resolution: 1 Kilometer

Built-up Land Projections

Description: The built up projection dataset includes the projected portion of each 1 kilometer grid cell that is built-up. Here, the definition of built-up is consistent with that of the Global Human Settlement Layer (see Section 2.1.2). The primary SSP2 dataset includes projections for each 10-year interval over the period 2020-2100. The three variants of SSP2 include projections for 2050 and 2100 only. For reference, the base-year (2014 observed GHSL) is included. The data are organized by country/region (regions are delineated in Annex A). Built-up land totals at the national-level for SSP2 and each variant are calculated separately, and downscaled to produce the spatial data layers (see Sections 2.2.5 and 2.2.8).

Source Files:

SSP2: Pop_builtup_projections_SSP2_2015_2100
Variants: Pop_Builtup_Variants_2050_2100

File names:

SSP2: XXX_BUProject_2015_2100.gdb\PopYEAR

XXX: Three character ISO code
YEAR: Four-digit year

Variants: XXX_BUProject_V_2050_2100.gdb\XXX_PopYEAR

XXX: Three character ISO code
V: Variant - will be one of three letters (H: High, M: Medium, L: Low)
YEAR: Four-digit year

File type: File Geodatabase Raster Dataset

Coordinate System: World Mollweide (EPSG:54009)

Spatial Resolution: 1 Kilometre